The Pennsylvania State University
The Graduate School

LOOP QUANTUM COSMOLOGY AND THE EARLY UNIVERSE

A Dissertation in
Physics
by
David Sloan

Submitted in Partial Fulfillment
of the Requirements
for the Degree of

Doctor of Philosophy

August 2010

The thesis of David Sloan was reviewed and approved* by the following:

Abhay Ashtekar
Eberly Professor of Physics
Dissertation Advisor, Chair of Committee

Martin Bojowald
Professor of Physics

Tyce De Young
Professor of Physics

Nigel Higson
Professor of Mathematics

Jayanth Banavar
Professor of Physics
Head of the Department of Physics

*Signatures are on file in the Graduate School.

Abstract

In this dissertation we explore two issues relating to Loop Quantum Cosmology (LQC) and the early universe. The first is expressing the Belinkskii, Khalatnikov and Lifshitz (BKL) conjecture in a manner suitable for loop quantization. The BKL conjecture says that on approach to space-like singularities in general relativity, time derivatives dominate over spatial derivatives so that the dynamics at any spatial point is well captured by a set of coupled ordinary differential equations. A large body of numerical and analytical evidence has accumulated in favor of these ideas, mostly using a framework adapted to the partial differential equations that result from analyzing Einstein's equations. By contrast we begin with a Hamiltonian framework so that we can provide a formulation of this conjecture in terms of variables that are tailored to non-perturbative quantization. We explore this system in some detail, establishing the role of 'Mixmaster' dynamics and the nature of the resulting singularity. Our formulation serves as a first step in the analysis of the fate of generic space-like singularities in loop quantum gravity.

The second issue is that of the role of inflation in LQC. In LQC the big bang singularity is replaced by a quantum bounce which is followed by a robust phase of super-inflation. We establish the behavior of effective equations for LQC in a generic setting then investigate in detail the particular case of early universe inflation caused by the slow roll of a scalar field down its potential. A natural measure is formed on the space of solutions to the equations of motion and it is established that in this scenario the *a priori* probability of seeing the required 68 efolds of inflation is in fact very high which stands in stark contrast to the results that have been presented in the classical case. In doing so we show that inflation in LQC suffers from no 'fine tuning' issue and is in fact a generic feature.

Table of Contents

List of Figures

Acknowledgments

The work in this Dissertation was supported in part by NSF grant PHY0854743, The George A. and Margaret M. Downsbrough Endowment, the Edward M. Frymoyer Scholarship, the Duncan Fellowship, and the Eberly research funds of the Pennsylvania State University. I am indebted to these sources for their generosity.

I owe a great deal of thanks to my advisor, Abhay Ashtekar who has acted as teacher, mentor and collaborator throughout my research. It is from Abhay that I have learned what it is to be a physicist.

I wish to also express my thanks for the support that I have received from the Institute for Gravitation and the Cosmos at Penn State. I have enjoyed and learned much from collaborations with Jonathan Engle, Adam Henderson, Tomas Liko and Andrew Randono. I have profited greatly from guidance and teaching from Martin Bojowald, Alex Corichi, Tomasz Pawlowski and Parampreet Singh.

I acknowledge and am grateful for useful interactions with my colleagues at Penn State, in particular Edward Wilson-Ewing, Miguel Campiglia, Victor Taveras, Artur Tsobanjan, William Nelson, Jacobo Diaz-Polo, Joseph Ochoa, Kevin Vandersloot, Mikhail Kagan, Nico Yunes, Juan Reyes, Simone Mercuri, Frank Herrmann, Ian Hinder, Florian Conrady, Dah-Wei Chiou, Casey Tomlin and David Simpson.

Finally I would be remiss in not thanking Randi Neshteruk for her extensive knowledge of academic procedures and untiring help in navigating bureaucracy. It takes someone with their feet firmly on the ground to support so many with their heads in the clouds.

Dedication

For my parents.

Ars sine scientia nihil est - Jean Mignot

Chapter 1

Introduction

From the inception of relativistic cosmology, it has been apparent that General Relativity admits singular solutions of physical interest. Initially the presence of singularities was the subject of a great deal of debate - some claimed that the presence of singularities was an artifact of the symmetries imposed on cosmological solutions and would not be present in more physically realistic solutions and in particular the Russian school believed that the singularity itself was not a true physical solution to the theory. This issue was ultimately laid to rest by the powerful singularity theorems of Penrose in 1965[1], which showed that singularities occur under very general conditions making them an essential feature of general relativity. However, despite showing that a singularities did indeed exist little was known about the dynamics of space-time near a generic singularity.

An alternate perspective on this is that the presence of a singularity is the result of applying the equations of General Relativity (GR) outside of their region of validity. In this viewpoint, GR is simply the low energy limit of a more complicated physical model. Indeed, since no physical test has been made in the high curvature regime, this idea cannot be ruled out. Several models have been produced which make classical corrections, mostly inspired by the idea that GR is non-renormalizable. Corrections to the Einstein-Hilbert action involving higher powers of the Ricci scalar or contractions of multiple copies of the Riemann tensor, the so-called '$f(R)$' theories[2], are amongst the more popular as by construction they can include GR as a low curvature limit.

The issue of singularities is of great importance in any approach to Quantum

Gravity. Singularities are an aesthetic issue in any physical theory, and one which it is expected that a deeper understanding of nature will resolve. It is deeply unsatisfying to consider that there is a point in time before which no further information can be known. It is to be hoped, therefore, that a more complete model will enable us to look beyond this horizon and extend our understanding of our past.

It is also expected that any complete theory of Quantum Gravity must agree with GR within the latter's range of validity. Deviations from the established theory are only to be expected at very high energy scales, and therefore singularities are our best hope of observing these deviations. Through understanding the classical approach to a singularity one can gain insight into which aspects of a quantum theory are the most relevant, and therefore what questions to ask of phenomenology. Thus singularities provide a window into the quantum world.

1.1 History of the Universe According to General Relativity

In 1922 Friedmann provided a homogeneous, isotropic solution to Einstein's equations [3]. Here the notion of dynamical space, as opposed to the absolute space of Newton was applied for the first time in cosmology. In this solution it was noticed that at finite time in the past the size of the universe shrank to zero, whilst the energy-density and curvature became infinite. Despite the presence of these features in Friedmann's model, their implications were first really understood by Lemaitre[4] - that they implied that the universe began with a singularity, dubbed the 'big bang'. In 1935 Robertson [5] and Walker [6] independently proved that Friedmann's metric described every cosmological scenario in which the vacuum speed of light is held constant. Although this is now widely accepted initially the idea that history ended to the distant past was considered unappealing - leading even Einstein to add a cosmological constant in an effort to yield a static universe.

According to what has now become the standard model of cosmology [1] the universe began with a big bang around 1.5×10^{10} years ago (in planck units,

[1]Here we use the term 'standard model' to mean widely accepted and not out of any reference to the standard model of physical interactions

5×10^{60} s_p ago). [2] This point is the past singularity of our cosmological solutions. From this point until the first planck second (10^{-42} seconds) little is known, as the universe was in the 'planck era' - during which it is assumed quantum mechanical effects dominated dynamics. There then followed, over the next 10^{-36} seconds (10^6 s_p) a period of 'inflation' in which the universe underwent an accelerated expansion. If one believes grand unification theories, then inflation must continue past the point of symmetry breaking of these theories and during the production of magnetic monopoles[60].

This epoch is followed by a period of reheating, when the inflaton decays into a relativistic plasma. This is the electroweak period[7] which takes place over the next 10^{-12} seconds (10^{30} s_p). After around 10^{-6} seconds (10^{36} s_p) quarks form, yet the temperature is still above that which would allow for hadron formation. At this point the four fundamental forces have become distinguishable.

Between 10^{-6} and 1 second (10^{42} s_p) the process of baryogenesis[8] begins and hadrons such as protons and neutrons form. At this point the cosmic neutrino background forms as neutrinos are now decoupled from other matter. This is followed over the next 10 seconds (10^{43} s_p) by a lepton dominated phase[9] which ends with lepton/anti-lepton annihilation producing a photon dominated regime[7]. During this regime, between 200 and 1000 seconds ($2 \times 10^{44} - 10^{45}$ s_p) nucleosynthesis[10] can occur producing hydrogen and helium nuclei. The photon dominated regime lasts for around $300,000$ years (10^{56} s_p). At the end of this period, the temperature is low enough that the first atoms can form, and the universe becomes transparent to photons. This is the point at which the Cosmic Microwave Background is formed giving us a picture of the universe at this time.

In this thesis we will discuss two aspects of this history from a perspective of Loop Quantum Cosmology. The first is an investigation of the BKL conjecture which posits a simplification of Einstein's equations applicable to regions in a close neighborhood of a singularity. The second is an examination of the phenomena of effective equations for LQC and the role of the inflationary epoch therein.

---

[2] We will denote the 'planck second' by $s_p = \sqrt{\frac{\hbar G}{c^3}}$ which is a convenient until when dealing in particular with quantum cosmology. Numbers given in this section are there to establish their orders of magnitude rather than exact values. Throughout this thesis we will work with planck units, obtained by setting $G = \hbar = c = 1$

1.2 The BKL Conjecture

In 1970, Belinskii, Khalatnikov and Lifshitz (BKL) made a conjecture which, if proven would shed considerable light on the nature of space-like singularities in GR: It is proposed that in the neighborhood of a singularity time derivatives would dominate over spatial derivatives, implying that the asymptotic dynamics would be well described by a series of coupled ordinary differential equations rather than partial differential equations. Although at first this appears an unlikely result, there is a growing body of evidence both analytic and numerical which supports this view.

Specifically the conjecture proposes that at any point in space the geometry is well described by the Bianchi I metric for long stretches of time periodically undergoing Bianchi II transitions. At specific points, gradients can grow, forming spikes, but the dynamics remains local.

It is now known in LQC that the Bianchi I and II singularities are resolved. This suggests that there may well be a general result which says that all space-like singularities of the classical theory are naturally resolved in loop quantum gravity. It is difficult to test this idea using the current formulations of the BKL conjecture since these approaches are motivated by the theory of partial differential equations rather than by Hamiltonian or quantum considerations. In particular, most approaches perform a rescaling of their dynamical variables by dividing by the trace of the extrinsic curvature. Such a procedure is difficult to reproduce in LQC as this would require an inverse extrinsic curvature operator. In the analysis presented here, we reformulate the BKL conjecture in a way more suited to loop quantization and explore the resulting system both analytically and numerically.

1.3 Effective Equations and their Implications

It has been observed both analytically and numerically that the effective equations for the simplest models of LQC closely match the full quantum dynamics not only in the infrared regime but throughout the entire evolution of the universe. This remarkable feature of the effective equations leads us to ask questions of their physical phenomena even away from these simple models to provide hints

as to where quantum effects should be manifest in the full theory. Through a careful analysis of the effective system of LQC we are able to show that there are signature features of these cosmologies in their full evolutions: Physical parameters such as the Hubble expansion rate and the total matter density remain bounded throughout an entire trajectory, attaining their bounds, and thus point towards where potential tests of the full theory may be performed.

It is also shown that under fairly generic conditions the effective system exhibits welcome geometrical features of a bouncing cosmology. The scalar curvature is bounded from above and the system undergoes a period of superinflation, a phenomenon not present in GR except in cases when energy conditions are broken or the matter action is non-minimally coupled. This superinflationary phase is generally short lived yet sufficient to connect contracting and expanding branches.

1.4 Loop Quantum Cosmology and Inflation

Inflationary models of the early universe have enjoyed a huge amount of success in explaining physical phenomena. The most striking result is a natural mechanism for structure formation. However, despite this success there is widespread concern that inflation requires 'fine tuning' of initial parameters - that one may have to require the state of the universe to be highly non-generic or chosen very carefully for sufficient inflation to occur. In particular, Gibbons and Turok have claimed that the probability of obtaining the required efolds in the expansion of the universe is suppressed by a number on the order of 10^{-88} - this would imply that further non-trivial input is required to explain how the universe came to be in such a state. However this calculation required a series of assumptions; since the space of solutions is non-compact space certain cut-offs or regularizations had to be imposed by hand.

In the LQC case, the corresponding space is in fact compact, a result that stems from the discreteness of the area parameter in Loop Quantum Gravity. Therefore LQC provides a system in which this calculation can be performed much more directly. In doing so we observe that the number of solutions exhibiting less than 68 efolds of inflation is negligible in comparison to those which inflate enough. Thus in the context of LQC coupled to a massive scalar field, inflation is a natural

mechanism through which the universe expands sufficiently, generically solving problems such as the overabundance of monopoles in the early universe.

Chapter 2

The BKL Conjecture

2.1 Introduction

Originally formulated by Belinskii, Khalatnikov, and Lifshitz in 1970 [12], the BKL conjecture states that as a space-like singularity is approached, time derivatives dominate over spatial derivatives. Thus partial differential equations are replaced by ordinary differential equations and the dynamics of GR become local and oscillatory, and with the significant exception of a scalar field, matter contributions become negligable - to quote Wheeler 'matter doesn't matter'. Thus each spatial point acts like a homogeneous cosmology, which were classified by Bianchi [13]. The simplest solutions being those with no intrinsic curvature, the Bianchi I metrics, and the next those with intrinsic curvature along one direction, the Bianchi II metrics. The BKL conjecture posits that the dynamics of each spatial point follow the 'Mixmaster' behavior - a sequence of Bianchi I solutions bridged by Bianchi II transitions. Initially this conjecture, based on a heuristic analysis on the Einstein field equations, was easy to dismiss as it appears coordinate dependent, breaking one of the fundamental tenets of General Relativity. [1]

Recently both numerical and analytic investigations have provided a great deal of support for this conjecture. Although there has not been significant progress towards a proof of the conjecture in the full theory there has been outstanding progress in simpler models. Berger[14], Garfinkle[15] Moncrief[16], Isenberg[17]

[1] This chapter follows the work of the author in [11].

and Weaver[18] showed that for a class of models the solutions to the Einstein field equations approach the 'Velocity Term Dominated' solutions obtained by neglecting spatial derivatives as the singularity is approached. Andersson and Rendall [19] have shown that for General Relativity coupled to a massless scalar field or a (VTD) stiff fluid even in the absence of symmetries for every solution to the VTD equations there exists a solution to the full field equations that converges to the VTD solution as the singularity is approached. In these VTD models the BKL behavior is simpler, allowing a precise statement of the conjecture that could be proven.

Numerical evolutions have provided the most convincing argument for the BKL conjecture to date. Berger and Moncrief began a program to analyze generic cosmological singularities [20]. Initially much work was done in symmetry reduced cases [21]. More Recently Garfinkle has performed numerical evolution of spacetimes with no symmetries in which again the Mixmaster behavior appears to be present.

In this chapter we will begin by expressing GR in 'first order' terms, and introduce a set of variables that are motivated by the BKL conjecture. The BKL conjecture is applied in the form of a truncation of our constraints and the resulting dynamics explored, establishing known features of Mixmaster dynamics such as the 'u-map' and spikes.

2.2 Preliminaries

We will consider spacetimes of the form ${}^4M = \mathcal{R} \times {}^3M$ where ${}^3M$ is a compact 3-dimensional manifold (without boundary). We will formulate GR in terms of first order variables, the basis of loop quantum gravity. These consist of pairs of fields consisting an orthonormal triad, $\widetilde{E}^a_i$ and its conjugate momentum K^i_a which on solutions will correspond to extrinsic curvature. The fundamental poisson bracket is given by

$$\{\widetilde{E}^a_i(x), K^j_b(y)\} = \delta^j_i \delta^a_b \delta^3(x-y) \tag{2.1}$$

Herein, early letters, a,b,c, denote spatial indices while i,j,k denote internal

indices which take values on $so(3)$ - the Lie algebra of $SO(3)$. Tildes are used to denote density weights of quantities; a tilde above indicates that the quantity transforms as a tensor density of weight 1. These variables are related to the older Arnowitt, Deser and Misner (ADM) counterparts by

$$\widetilde{E}^a_i \widetilde{E}^b_j \eta^{ij} = q q^{ab} \tag{2.2}$$

$$K^i_a \widetilde{E}^b_i = \sqrt{q} K_a{}^b \tag{2.3}$$

where q_{ab} is the metric on the leaf ${}^3M$, q its determinant, and K_{ab} the extrinsic curvature of ${}^3M$.

In terms of these variables we perform a 3+1 decomposition of space-time in which our Hamiltonian is [23]

$$H[\widetilde{E}, K] = -\int_{{}^3M} \frac{1}{2} \underset{\sim}{N} \widetilde{\widetilde{S}} + \frac{1}{2} N^a \widetilde{V}_a + ({}^4A \cdot t)^{ij} \widetilde{G}_{ij} \tag{2.4}$$

which is a sum of constraints with Lagrange multipliers. The Lagrange multipliers $\underset{\sim}{N}$,$\underset{\sim}{N}^a$, the lapse and shift, are related to the choice of slicing and time. $({}^4A \cdot t)^{ij}$ is related to rotations in the internal space. The constraints $\widetilde{\widetilde{S}}$, $\widetilde{V}_a$, and $\widetilde{G}_{ij}$ are the scalar, vector, and Gauss constraints respectively. The constraints are [23]

$$\widetilde{\widetilde{S}} \equiv -q\mathcal{R} - 2\widetilde{E}^a_{[i} \widetilde{E}^b_{j]} K^i_a K^j_b \tag{2.5}$$

$$\widetilde{V}_a \equiv 4 \widetilde{E}^b_i D_{[a} K^i_{b]} \tag{2.6}$$

$$\widetilde{G}_{ij} \equiv -\widetilde{E}^a_{[i} K_{aj]} \tag{2.7}$$

Where $\mathcal{R}$ is the scalar curvature of the derivative operator D_a compatible with the metric q_{ab}. The overall sign and numerical factors in the constraints are chosen so they reduce to the ADM constraints upon solving the Gauss constraint. $\mathcal{R}$ can be written in terms of the triad and its inverse or in terms of the triad and the connection compatible with the triad Γ^i_a.

$$D_a\widetilde{E}^b_i + \epsilon_{ijk}\Gamma^j_a\widetilde{E}^{bk} = 0 \tag{2.8}$$

$$\Gamma^j_a = -\frac{1}{2}\underset{\sim}{E}_{bk}D_a\widetilde{E}^b_i\epsilon^{ijk} \tag{2.9}$$

The equations of motion are obtained by taking Poisson brackets with the Hamiltonian.

$$\dot{\widetilde{E}}^a_i = \{\widetilde{E}^a_i, H[\widetilde{E}, K]\} \tag{2.10}$$

$$\dot{K}^i_a = \{K^i_a, H[\widetilde{E}, K]\} \tag{2.11}$$

The phase space variables that form the basis of loop quantum gravity can be simply obtained from $\{E^a_i, K^i_a\}$ by a canonical transformation.

$$\{\widetilde{E}^a_i, K^i_a\} \to \{A^i_a, \gamma^{-1}\widetilde{E}^i_a\} \tag{2.12}$$

$$A^i_a = \Gamma^i_a + \gamma K^i_a \tag{2.13}$$

For clarity of presentation we will work with the phase space $(\widetilde{E}^a_i, K^i_a)$.

2.3 BKL Motivated Variables

It is not immediately apparent how to apply the BKL conjecture in terms of this Hamiltonian formulation. A number of questions immediately arise: What kind of derivatives dominate as one approaches the singularity and what kind become negligible? Derivatives of what quantities are to become negligible? A framework due to Uggla, Ellis, Wainwright and Elst (UEWE)[24] gives a rigorous statement of what the BKL conjecture is by answering these questions in the ADM formalism. Applying the conjecture to their equations of motion they obtain a simplified systems that successfully describes the expected oscillatory BKL behavior. Further their form of the BKL conjecture is supported by numerical evolutions. We will motivate the definition of our variables and our form of the conjecture from their

framework.

Drawing motivation from the scale-invariant framework of Uggla, et al [25] we define a set of variables that are adapted to describe the BKL conjecture and that are suitable for quantization. Of particular use in this framework is a 'Hubble normalized triad' $K^{-1}e^a_i$ which is expected to become degenerate at the singularity. From this the 'scale invariant variables' are formed:

$$\Sigma_{ij} = 3K^{-1}e^a_i K_{aj} - K^{-1}e^a_k K^k_a \delta_{ij} \tag{2.14}$$

$$N_{ij} = -3K^{-1}e^a_{(i}\Gamma_{aj)} + 3K^{-1}e^a_k \Gamma^k_a \delta_{ij} \tag{2.15}$$

$$A_i = -\epsilon_i{}^{jk} 3K^{-1}e^a_j \Gamma^k_a \tag{2.16}$$

$$\partial_i = 3K^{-1}e^a_i \partial_a \tag{2.17}$$

It is expected that these variables will remain finite at the singularity [26] due to the division by the trace of the extrinsic curvature, and that the derivative introduced will become negligible when acting upon these variables. We aim to produce a similar set, but will diverge from their motivation of scale invariance for two reasons: The first is that dividing quantities by the trace of the extrinsic curvature, K, is not natural for quantization, since it is difficult to define an operator corresponding to $\frac{1}{K}$. Using only products and sums of phase space variables it is not possible to construct scale invariant scalar quantities. The second is that although scale invariant quantities that can be constructed,K^i_a and Γ^i_a, but are typically divergent at singularities. We will motivate our framework from the properties of the Hubble normalized triad $K^{-1}e^a_i$. We argue that it is the degeneracy of the Hubble normalized triad at the singularity that suppresses derivatives and gives bounded variables at the singularity.

The densitized triad, $\widetilde{E}^a_i = \sqrt{q}e^a_i$ has similar properties to the Hubble normalized triad. Since $\sqrt{q}$ approaches zero near a typical space-like singularity we expect that $\widetilde{E}^a_i = \sqrt{q}e^a_i$ will be degenerate near the singularity as well. We will therefore motivate our construction from this, however the resulting system is a precise, self-contained conjecture. We find that in examples the properties we seek are realized; for the vacuum Bianchi I solution with lapse $N = 1$ the densitized

and Hubble normalized triads have the some time dependence, since

$$\widetilde{E}_i^a = \frac{\widetilde{K}}{3} E_i^a \tag{2.18}$$

$$\widetilde{K} = 1 \tag{2.19}$$

More generally if $\widetilde{K}$ is bounded as the singularity is approached then the densitized triad will be degenerate if and only if the Hubble-normalized triad is.

We construct scalar densities by contracting $\widetilde{E}_i^a$ with K_a^i, and Γ_a^i.

$$\widetilde{P}_i{}^j = \widetilde{E}_i^a K_a^j - \widetilde{E}_k^a K_a^k \delta_i{}^j \tag{2.20}$$

$$\widetilde{C}_i{}^j = \widetilde{E}_i^a \Gamma_a^j - \widetilde{E}_k^a \Gamma_a^k \delta_i{}^j \tag{2.21}$$

An important feature of these variables is that they are tensors with *only internal indices* . Under diffeomorphisms $\widetilde{P}$ and $\widetilde{C}$ transform as densitized scalars. Notice that $\widetilde{P}_{ij}$ bears a close resemblance to the P_{ab}, the ADM momentum. These variables are related to the scale invariant variables of Uggla et al by:

$$\Sigma_{ij} = -\frac{6\widetilde{P}_{ij}}{\widetilde{P}} + 2\delta_{ij} \tag{2.22}$$

$$N_{ij} = -\frac{\widetilde{C}_{ij}}{\widetilde{P}} \tag{2.23}$$

Our scalar density variables $\widetilde{P}_{ij}$ and $\widetilde{C}_{ij}$ are again bounded if $\widetilde{K}$ is bounded as the singularity is approached.

We further define

$$\widetilde{D}_i = \widetilde{E}_i^a D_a. \tag{2.24}$$

These $\widetilde{D}_i$ will be the spatial derivatives we consider negligible near the singularity. This operator is linear and Liebnitz, but due to its action on functions

$$\widetilde{D}_i f = \widetilde{E}_i^a \partial_a f \tag{2.25}$$

$\widetilde{D}_i$ is not a connection, however if treated as a connection it has interesting features.

The connection has torsion, which is related to $\widetilde{C}$.

$$\widetilde{D}_{[i}\widetilde{D}_{j]}f = -\epsilon_{kl[i}\widetilde{C}_{j]}{}^{l}\widetilde{D}^{k}f = -\widetilde{T}^{k}{}_{ij}\widetilde{D}_{k}f \tag{2.26}$$

$$\widetilde{T}^{k}{}_{ij} = \epsilon_{kl[i}\widetilde{C}_{j]}{}^{l} \tag{2.27}$$

We can rewrite the constraints in terms of the densitized triad and these scalar density variables.

$$\widetilde{\widetilde{S}} = 2\epsilon^{ijk}\widetilde{D}_{i}(\widetilde{C}_{jk}) + 4\widetilde{C}_{[ij]}\widetilde{C}^{[ij]} + \widetilde{C}_{ij}\widetilde{C}^{ji} - \frac{1}{2}\widetilde{C}^{2} + \widetilde{P}_{ij}\widetilde{P}^{ji} - \frac{1}{2}\widetilde{P}^{2} \approx 0 \tag{2.28}$$

$$\widetilde{\widetilde{V}}_{i} = \widetilde{E}^{a}_{i}\widetilde{V}_{a} = -2\widetilde{D}_{j}\widetilde{P}_{i}{}^{j} + 2\epsilon_{jkl}\widetilde{P}^{kl}(\widetilde{C}_{i}{}^{j} - \widetilde{C}\delta_{i}{}^{j}) - \epsilon_{ijk}\widetilde{C}^{jk}\widetilde{P} + 2\epsilon_{ijk}\widetilde{P}^{jl}\widetilde{C}_{l}{}^{k} \approx 0 \tag{2.29}$$

$$\widetilde{G}_{ij} = -\widetilde{P}_{[ij]} \approx 0 \tag{2.30}$$

Here we have contracted the vector constraint with a densitized triad to obtain a constraint $\widetilde{\widetilde{V}}_{i}$. Since the triad is assumed to be invertible everywhere except at the singularity, this constraint defines the same surface as the original vector constraint $\widetilde{V}_{a}$. By defining this new constraint $\widetilde{\widetilde{V}}_{i}$ the terms in each constraint can be grouped into two classes defined as follows. Let us define Π_{n} to be the set of polynomials of order n in $\widetilde{C}, \widetilde{P}$, and $\underset{\sim}{N}$ and $D\Pi_{m}$ to be elements in the set of polynomials of order m in $\widetilde{C}, \widetilde{P}, \underset{\sim}{N}, \widetilde{D}$ containing at least one derivative $\widetilde{D}$. Each constraint can then be decomposed into a sum of terms in Π_{2} and terms in $D\Pi_{2}$. This feature will motivate our form the BKL conjecture. The equations of motion for $\widetilde{E}^{a}_{i}$, $\widetilde{C}_{ij}$, $\widetilde{P}_{ij}$ can be written in a similar form.

$$\dot{\widetilde{\widetilde{C}}}^{ij} = \epsilon^{jkl}\widetilde{D}_{k}(\underset{\sim}{N}(1/2\delta^{i}_{l}\widetilde{P} - \widetilde{P}_{l}{}^{i})) - \underset{\sim}{N}[2\widetilde{C}^{(i}_{k}\widetilde{P}^{|k|j)} + 2\widetilde{C}^{[kj]}\widetilde{P}_{k}{}^{i} - \widetilde{P}\widetilde{C}^{ij}] \tag{2.31}$$

$$\begin{aligned}\dot{\widetilde{\widetilde{P}}}^{ij} = {} & -\epsilon^{jkl}\widetilde{D}_{k}(\underset{\sim}{N}\widetilde{C}_{l}{}^{i}) + \frac{1}{2}\epsilon^{ijk}\widetilde{D}_{k}(\underset{\sim}{N}\widetilde{C}) - \epsilon^{klm}\widetilde{D}_{m}(\underset{\sim}{N}\widetilde{C}_{kl})\delta^{ij} \\ & + 2\epsilon^{jkm}\widetilde{C}^{[ik]}\widetilde{D}_{m}(\underset{\sim}{N}) + (\widetilde{D}^{i}\widetilde{D}^{j} - \widetilde{D}^{k}\widetilde{D}_{k}\delta^{ij})\underset{\sim}{N} \\ & + \underset{\sim}{N}[-2\widetilde{C}^{(ik)}\widetilde{C}_{k}{}^{j} + \widetilde{C}\widetilde{C}^{ij} + 2\widetilde{C}^{[kl]}\widetilde{C}_{[kl]}]\delta^{ij}\end{aligned} \tag{2.32}$$

$$\dot{\widetilde{E}}^{a}_{i} = -\underset{\sim}{N}\widetilde{P}_{i}{}^{j}\widetilde{E}^{a}_{j} \tag{2.33}$$

We have set the shift to zero to reduce clutter. The equations of motion for $\widetilde{P}_{ij}$ and $\widetilde{C}_{ij}$ can again be decomposed into two groups of terms; those in $\underset{\sim}{N}\Pi_{3}$, and

those in $\underset{\sim}{N}D\Pi_3$ or $D_iD_j\underset{\sim}{N}$. With zero shift the equation of motion for $\widetilde{E}^a_i$ is a simple linear equation. The constraints and equations of motion for $\widetilde{C}_{ij}$ and $\widetilde{P}_{ij}$ can then be written in terms scalar density variables and the derivative $\widetilde{D}_i$. Our form of the BKL conjecture is then motivated to be that terms in Π_n dominate those in $D\Pi_n$.

These equations of motion can be derived by taking Poisson brackets with the Hamiltonian. To simplify this process the Poisson brackets between $\widetilde{E}^a_i$, $\widetilde{C}_{ij}$, and $\widetilde{P}_{ij}$ can be derived

$$\{\widetilde{E}^a_i, \widetilde{P}_{jk}\} = \widetilde{E}^a_j\delta_{ik} - \widetilde{E}^a_i\delta_{jk} \tag{2.34}$$

$$\{\widetilde{P}_{ij}, \widetilde{P}_{kl}\} = \widetilde{P}_{kj}\delta_{il} - \widetilde{P}_{il}\delta_{kj} \tag{2.35}$$

$$\{\int f_{ij}\widetilde{P}^{ij}, \int g_{kl}\widetilde{C}^{kl}\} = \int f_{ij}g_{kl}(\widetilde{C}^{kj}\delta^{il} + \widetilde{C}^{jl}\delta^{ik}) + \epsilon^{jlm}\delta^{ik}g_{kl}\widetilde{D}_m f_{ij} \tag{2.36}$$

We notice here that the $\widetilde{P}_{ij}$ have the same algebra as $GL(3,\mathbb{R})$. From the Poisson bracket $\widetilde{C}_{ij}$ and $\widetilde{P}_{ij}$ we see that $\widetilde{C}_{ij}$ transforms as a connection under $GL(3,\mathbb{R})$ transformations.

This formulation is applicable outside of just describing the BKL conjecture. The evolution equations and constraints do not depend on the inverse triad, except through the definition of $\widetilde{C}$. If initial data is then chosen that solves the constraints as well as the constraint relating the densitized triad to $\widetilde{C}$ then this data can be evolved to the point where the triad is degenerate. Further we expect that in evolving towards the singularity the triad becomes degenerate. By contracting the quantities that often diverge at singularities, K^i_a, Γ^i_a, the quantities $\widetilde{C}_{ij}$, $\widetilde{P}_{ij}$ remain bounded or have a much lower degree of divergence. Since our equations of motion do not involve the inverse triad, E^i_a the degeneracy of the triad is not an issue - in many instances the variables we define will remain finite through the singularity.

2.4 Truncation

Since our equations of motion and constraints can be decomposed into the sum of terms in $D\Pi_n$ and Π_n we are naturally lead to examine a truncation of the full theory in which we set all elements of $D\Pi_n$ to zero. In doing so we will retain only those terms in Π_n - the terms we expect to become dominant at the singularity.

We therefore formulate the BKL conjecture to be:

- $\exists X \in \Pi_n$ such that $\forall Y \in D\Pi_n, \frac{Y}{X} \to 0$ as we approach the singularity.
- $\widetilde{C}$ and $\widetilde{P}$ remain bounded near the singularity.
- $\underset{\sim}{N}$ and $\underset{\sim}{N}^i$ remain bounded near the singularity.
- The full dynamics is well approximated by setting terms in $D\Pi_n$ to zero.

The terms in $D\Pi_n$ may tend to zero either due to terms in Π_n becoming homogeneous or because the triad is becoming degenerate. If the triad is becoming degenerate the covariant derivatives of $\widetilde{P}$ and $\widetilde{C}$ can be non-zero, but near the singularity they are being suppressed by the triad. The finiteness of $\widetilde{P}$ and $\widetilde{C}$ ensures that products of these variables with derivative terms will still tend to zero as the singularity is approached. The restriction of the finiteness of $\underset{\sim}{N}$ and $\underset{\sim}{N}^i$ moves the singularity infinitely far away.

If we asssume this conjecture holds we can truncate the full theory by setting derivative terms to zero.

The truncated theory is defined by

$$\widetilde{D}_i\widetilde{C}_{jk} = \widetilde{D}_i\widetilde{P}_{jk} = \widetilde{D}_i\underset{\sim}{N} = \widetilde{D}_i\underset{\sim}{N}_j = \widetilde{C}_{[ij]} = 0 \tag{2.37}$$

This defines a subspace of the full phase space, which we will call the truncated subspace. The section of this phase space containing non-degenerate triads consists of homogeneous $\widetilde{C}$ and $\widetilde{P}$. If we extend the phase space to include degenerate triads then the section of the truncated subspace containing degenerate triads consists of $\widetilde{C}$ and $\widetilde{P}$ which are homogeneous along the directions defined by the non-degerate part of the triad, but are free to vary along the degenerate directions. The lapse and shift are also constrained by to homogeneous along the non-degenerate directions of the triad. The truncated subspace the becomes the union of the homogeneous subspace with boundary of phase space consisting of degenerate triads.

This subspace is invariant under the full dynamics. If the derivatives terms are initially zero they will remain zero under the full equations of motion. This should be a necessary criterion for the BKL behavior because we expect the BKL behavior

to be described by the dynamics approaching some fixed point as is discussed in the work of Uggla.

The Poisson bracket between $\widetilde{P}$ and $\widetilde{C}$ can be simplified in this truncation. The smearings f_{ij} and g_{ij} will in general be constructed from the available fields with internal indices - in general they must be members of at least Π_1 such as $(\widetilde{D}_i, \widetilde{C}_{ij}, \widetilde{P}_{ij}, \underset{\sim}{N}, \underset{\sim}{N}_i, \eta_{ij})$ When evaluating the Poisson brackets the terms containing derivative of the smearing are then set to zero in the truncation. The truncated Poisson brackets between $\widetilde{C}$ and $\widetilde{P}$ are

$$\{\widetilde{P}_{ij}, \widetilde{C}_{kl}\}_T = \widetilde{C}_{kj}\delta_{il} + \widetilde{C}_{jl}\delta_{ik} \tag{2.38}$$

$$\left\{\widetilde{P}_{ij}, \widetilde{P}_{kl}\right\}_T = \widetilde{P}_{kj}\delta_{il} - \widetilde{P}_{il}\delta_{kj} \tag{2.39}$$

$$\left\{\widetilde{C}_{ij}, \widetilde{C}_{kl}\right\}_T = 0 \tag{2.40}$$

The constraints can be simply truncated to obtain

$$\widetilde{\widetilde{S}}_T = \quad \widetilde{C}_{ij}\widetilde{C}^{ji} - \frac{1}{2}\widetilde{C}^2 + \widetilde{P}_{ij}\widetilde{P}^{ji} - \frac{1}{2}\widetilde{P}^2 \approx 0 \tag{2.41}$$

$$\widetilde{\widetilde{V}}_{i(T)} = \quad 2\epsilon_{jkl}\widetilde{P}^{kl}(\widetilde{C}_i{}^j - \widetilde{C}\delta_i{}^j) + 2\epsilon_{ijk}\widetilde{P}^{jl}\widetilde{C}_l{}^k \approx 0 \tag{2.42}$$

$$\widetilde{G}_{ij(T)} = \quad -\widetilde{P}_{[ij]} \approx 0 \tag{2.43}$$

It is interesting to note here certain features of our constraints. The scalar constraint is symmetric in $\widetilde{C}$ and $\widetilde{P}$ - this symmetry will be broken at the level of equations of motion as the Poisson algebra is not symmetric. Also note that by adding a multiple of the Gauss constraint to the vector constraint can reformulate our constraints (with the exception of the Gauss constraint) to be completely symmetric in $\widetilde{C}$ and $\widetilde{P}$:

$$\widetilde{\widetilde{V'}}_{i(T)} = \epsilon_{ijk}\widetilde{P}^{jl}\widetilde{C}_l{}^k \approx 0 \tag{2.44}$$

We can consider $\widetilde{C}$ and $\widetilde{P}$ as matrices, being tensors of only internal indices and hence acting as scalars under diffeomorphisms. This constraint, $\widetilde{\widetilde{V'}}_{i(T)}$ implies that $\widetilde{C}$ and $\widetilde{P}$ commute. The Gauss constraint has no corresponding constraint

on $\widetilde{C}$, however as has been shown above consistency of this truncation requires that $\widetilde{C}$ be symmetric. Therefore if we solve the Gauss constraint we find that our constraint system is symmetric.

The truncated equations of motion can be obtained in two ways: First by applying the truncation to the full equations of motion by setting derivative terms to zero. Second they can be obtained by taking truncated Poisson brackets with truncated Hamiltonian.

$$\dot{f}_T = \{f, H_T\}_T \tag{2.45}$$

Where the truncated Hamiltonian is defined by

$$H[\widetilde{C}, \widetilde{P}]_{(T)} = \int_\Sigma \frac{1}{2}\underset{\sim}{N}\widetilde{\widetilde{S}}_T - \frac{1}{2}\underset{\sim}{N}^i\widetilde{V}_{(T)} - ({}^4A \cdot t)^{ij}\widetilde{G}_{ij(T)} \tag{2.46}$$

From which we find the equations of motion:

$$\dot{\widetilde{C}}^{ij} = -\underset{\sim}{N}[2\widetilde{C}^{(i}{}_k\widetilde{P}^{|k|j)} - \widetilde{P}\widetilde{C}^{ij}] \tag{2.47}$$

$$\dot{\widetilde{P}}^{ij} = \underset{\sim}{N}[2\widetilde{C}^{ik}\widetilde{C}_k{}^j - \widetilde{C}\widetilde{C}^{ij}] \tag{2.48}$$

$$\dot{\widetilde{E}}^a_i = \underset{\sim}{N}\widetilde{P}_i{}^j\widetilde{E}^a_j \tag{2.49}$$

A question arises here as to the consistency of our scheme - at what level do we apply this truncation of the theory? For an example, consider the FLRW space-times. There we consider space to be homogeneous and isotropic and impose this symmetry on the system at the level of constraints. If, however the symmetry did not hold over to the equations of motion, so that a space-time which has initial symmetry evolved away from the symmetric sector the reduction would have no meaning. Likewise, if an imposition of symmetry at the level of equations of motion did not give rise to the same system as the imposition at the level of constraints, the resulting sector would be ill-defined as there would be no agreement over what could be called the symmetric sector. The question which we must address is similar: Does the truncation of constraints lead us to the same system as truncation of the full equations of motion? The answer is in the affirmative. This fact is illustrated by the following 'commutativity diagram':

$$\begin{array}{ccc} \text{Full Constraint} & \xrightarrow{\text{Truncation}} & \text{Truncated Constraint} \\ \Big\downarrow \text{Equation of Motion} & & \Big\downarrow \text{Equation of Motion} \\ \text{Full Equation of Motion} & \xrightarrow{\text{Truncation}} & \text{Truncated Equation of Motion} \end{array}$$

The equations of motion for $\widetilde{C}$ and $\widetilde{P}$ depend only on $\widetilde{C}$,$\widetilde{P}$, and the lapse and shift. There is then a closed system expressed *entirely in terms of* $\widetilde{C}$ *and* $\widetilde{P}$. The triad entirely decouples from the evolution. Therefore one can first solve the equations of motion for $\widetilde{C}$ and $\widetilde{P}$ and then evolve the triad afterwards. We then take this closed system in terms of $\widetilde{P}$ and $\widetilde{C}$ and consider it to be the Hamiltonian system describing the BKL conjecture. The phase space is coordinatized by $\widetilde{P}$ and $\widetilde{C}$ with Poisson brackets defined above.

Furthermore the truncated system forms a fixed subspace of the full phase space. Consider the subspace defined by $X = 0 \ \forall X \in D\Pi_n$. The equations of motion from the full theory leave this subspace invariant, that is all elements of $D\Pi_n$ will remain zero. Therefore in this subspace the truncated theory reproduces exactly the full theory. It is also worth noting here that this subspace contains many space-times of interest, particularly all the Bianchi type A models.

2.5 Reduced Phase Space

The truncated theory in terms of $\widetilde{C}$ and $\widetilde{P}$ can be gauge fixed using the Gauss and vector constraints. Should mention what the constraints are first and then how they restrict $\widetilde{C}$ and $\widetilde{P}$ then what transformations they generate. The infinitesimal transformations generated by the Gauss constraint are

$$\{\widetilde{P}_{ij}, \int \Lambda^{kl} G_{kl}\} = \Lambda_i{}^k \widetilde{P}_{kj} + \Lambda_j{}^k \widetilde{P}_{ik} \tag{2.50}$$

$$\{\widetilde{C}_{ij}, \int \Lambda^{kl} G_{kl}\} = \Lambda_i{}^k \widetilde{C}_{kj} + \Lambda_j{}^k \widetilde{C}_{ik} \tag{2.51}$$

As expected the Gauss constraint generates internal $SO(3)$ rotations. Instead of working directly with the vector constraint we will modify it by removing the terms proportional to the Gauss constraint. We define therefore define V'

$$\widetilde{\widetilde{V'}}_{i(T)} = 2\epsilon_{ijk}\widetilde{P}^{jl}\widetilde{C}_l{}^k \approx 0 \tag{2.52}$$

This constraint generates the following infinitesimal transformations

$$\{\widetilde{P}_{ij}, \int \underset{\sim}{N}^k \widetilde{\widetilde{V'}}_{k(T)}\} \approx 4\underset{\sim}{N}^k[\epsilon_{klm}\widetilde{C}_{(i}{}^m\widetilde{P}_{j)}{}^l + \epsilon_{kl(i}\widetilde{P}_{j)}{}^n\widetilde{C}_n{}^l] \tag{2.53}$$

$$\{\widetilde{C}_{ij}, \int \underset{\sim}{N}^k \widetilde{\widetilde{V'}}_{k(T)}\} \approx -4\underset{\sim}{N}^k[\epsilon_{kl(i}\widetilde{C}_{j)}{}^m\widetilde{C}_m{}^l] \tag{2.54}$$

Solving the Gauss and Vector constraints implies that $\widetilde{P}$ is symmetric and commutes with $\widetilde{C}$. We can then choose a basis such that $\widetilde{P}$ and $\widetilde{C}$ are simultaneously diagonalized. Looking at the action of the constraints on $\widetilde{P}$ and $\widetilde{C}$ we see that this is not preserved - moving along the gauge orbit takes us off the surface defined by diagonal $\widetilde{P}$ and $\widetilde{C}$, thus our diagonalization *fixes* our choice of gauge.

The Poisson brackets of the gauge fixed subspace are

$$\{P_I, P_J\} = \{C_I, C_J\} = 0 \tag{2.55}$$

$$\{P_I, C_J\} = 2\delta_{IJ}C_J \tag{2.56}$$

After gauge fixing the Hamiltonian and equations of motion take the form

$$\frac{1}{2}\left(\sum_I C_I\right)^2 - \sum_I C_I^2 + \frac{1}{2}\left(\sum_I P_I\right)^2 - \sum_I P_I^2 = 0 \tag{2.57}$$

$$\dot{P}_I = \underset{\sim}{N}C_I\left(\sum_J C_J - 2C_I\right) \tag{2.58}$$

$$\dot{C}_I = -\underset{\sim}{N}C_I\left(\sum_J P_J - 2P_I\right) \tag{2.59}$$

We arrive at a very simple system which can be easily simulated. The following are the results of a numerical simulation of this system, the details of which are in appendix A.

In the figures 2.1 and 2.2 we begin our evolution with the eigenvalues of C set

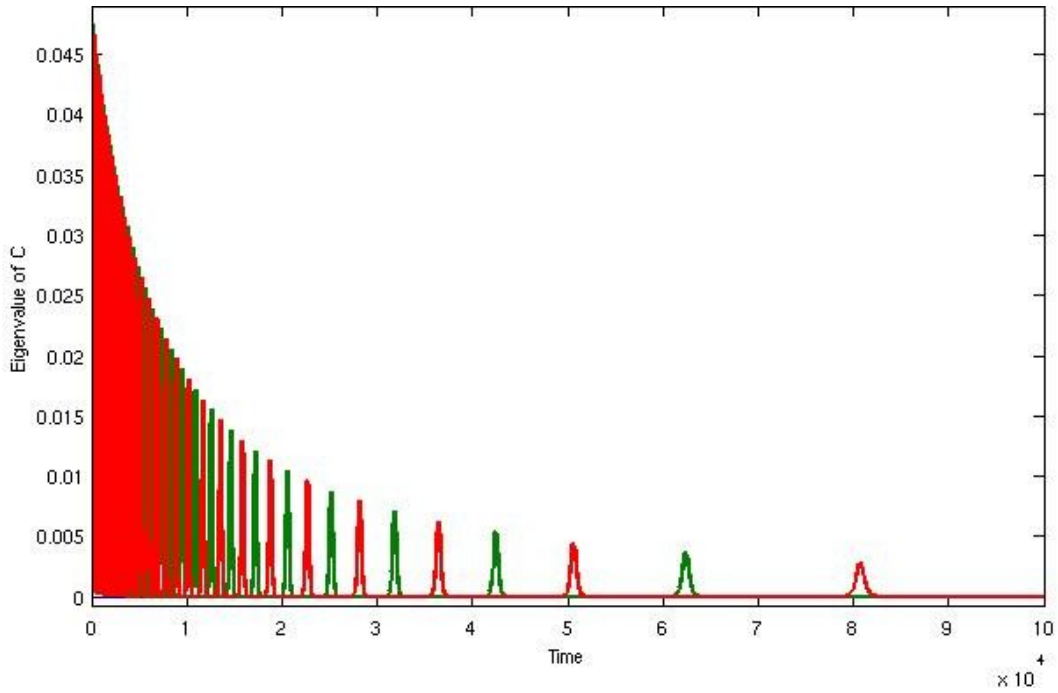

Figure 2.1. Evolution of each of the eigenvalues of C (C1 in red, C2 green, C3 blue) over time, in which we see a series of separate Taub transitions between Kasner states

to be $\{1.5, 0.004, 0.007\}$ and P set to $\{-0.47, -1.3, -1.4\}$.

2.6 Introduction of a Scalar Field

Until now, our analysis has been performed entirely on the vacuum theory. We can extend our system to include matter in a fairly simple manner by refining our model via the Hamiltonian to be:

$$H = H_{GR} + H_{matter} \tag{2.60}$$

The form of matter of particular interest to us will be that of a (massless) scalar field. This system has been analyzed in detail by Andersson and Rendall who have shown that in the presence of a scalar field with momentum above some minimum value the dynamics of space-time reduces to a single Kasner epoch. A massless scalar field is also used extensively in Loop Quantum Cosmology to define a clock variable. The Hamiltonian, H_{matter} in that case becomes $H_{SF} = \frac{\pi^2}{2} + \eta^{IJ} D_I\phi D_j\phi$.

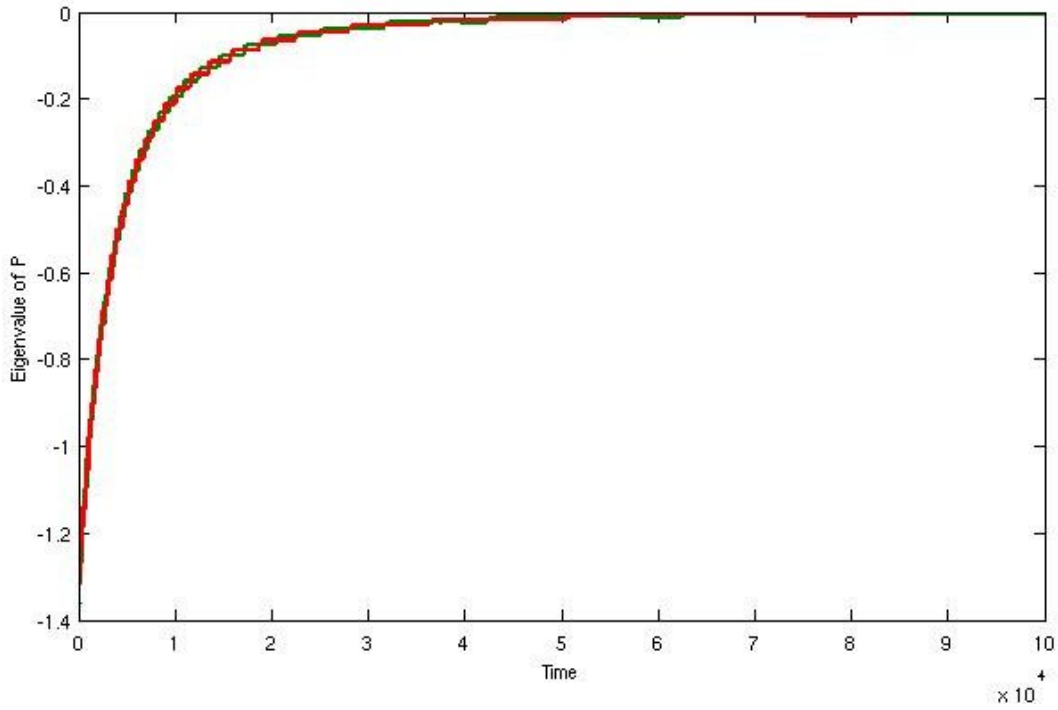

Figure 2.2. Evolution of the eigenvalues of P (P1 red, P2 green, P3 blue) over time. The largest eigenvalue transits the second, with all three tending to zero over time.

The analysis of section 2.5 follows almost exactly if we add the field ϕ to the set Π. The truncated constraints remain as above, except for 2.46 which gains a term $\frac{\pi^2}{2}$, which in turn refines the fully reduced Hamiltonian, 2.57 to become:

$$\frac{1}{2}\left(\sum_I C_I\right)^2 - \sum_I C_I^2 + \frac{1}{2}\left(\sum_I P_I\right)^2 - \sum_I P_I^2 + \frac{\pi^2}{2} \tag{2.61}$$

Wherein we recover the equations of motion for C and P as above, along with:

$$\dot{\phi} = \pi \quad \dot{\pi} = 0 \tag{2.62}$$

Although we have not altered the equations of motion for C and P, we have altered the solutions to our Hamiltonian constraint and hence we find a different resulting set of space-times. Of particular interest are the Bianchi I solutions to this system. Here we find that space-time takes the form

$$ds^2 = -d\tau^2 + \tau^{2p_x}dx^2 + \tau^{2p_y}dy^2 + \tau^{2p_z}dz^2 \tag{2.63}$$

on which $p_x + p_y + p_z = 1$ and the Hamiltonian constraint sets

$$p_x^2 + p_y^2 + p_z^2 = 1 - \pi^2 \tag{2.64}$$

These two relations define a one-parameter space of solutions - the intersection of a sphere and a plane. For $\pi^2 < \frac{1}{2}$ we find that solutions exist only if one of the values of p_i is negative, and this leads to an instability of the solution which is discussed below. However for $\pi^2 > \frac{1}{2}$ we find that all the p_i are positive and hence the solution is stable. In the vacuum case it is convenient to solve the constraints to express the p_i in terms of a single parameter u. Without loss of generality we take $u > 1$ and parameterize the space of p_i by:

$$p_1 = \frac{u^2 + u}{1 + u + u^2} \tag{2.65}$$

$$p_2 = \frac{u + 1}{1 + u + u^2} \tag{2.66}$$

$$p_3 = \frac{-u}{1 + u + u^2} \tag{2.67}$$

Our where p_1, p_2, p_3 are the set p_x, p_y, p_z in descending order. This parametrization will later form the basis of the 'u-map' relating transitions between Kasner states.

2.7 Analysis of Reduced Phase Space

We can analyze these reduced equations as a dynamical system as in Uggla et al [24]. We first identify fixed points of the dynamics for which

$$\dot{c_I} = \dot{p_I} = 0 \tag{2.68}$$

There are only two sets of fixed points for these equations.

1. $c_I = 0$ and $\sum_I p_I^2 - \frac{1}{2}\left(\sum_I p_I\right)^2 = 0$

2. $c_1 = c_2$,$c_3 = 0$, $p_1 = p_2$, $p_3 = 0$

The first fixed set of fixed points are the Kasner solutions. The second set of fixed points are highly unstable, being essentially a dimensional reduction of our theory [25]. We perturb away from these fixed points and obtain evolution equations for the perturbations. For the first fixed point the solutions to the constraint

$$\sum_I p_I^2 - \frac{1}{2}\left(\sum_I p_I\right)^2 = 0 \tag{2.69}$$

are all positive or all negative p_I. Since we want to analyze solutions that approach the singularity as $t \to \infty$ we restrict our attention to the solutions with positive p_I. If we perturb from a Kasner fixed point,

$$p_I' = p_I + \delta p_I \tag{2.70}$$

$$c_I' = c_I + \delta c_I \tag{2.71}$$

the evolution equations for the perturbations are

$$\dot{\delta p_I} = \mathcal{O}(\delta p^2) \tag{2.72}$$

$$\dot{\delta c_I} = -\underset{\sim}{N}\delta c_I(\sum_J p_J - 2p_I) + \mathcal{O}(\delta c \delta p) \tag{2.73}$$

The constraint on the p_I ensures that for a solution approaching the singularity one c_I is unstable under perturbations while the other two are stable. We can take p_1 to be the largest of the p_I's initially which implies that it can c_1 are unstable under perturbations. The evolution equations for c_1, p_1 assuming the other variables remain at their fixed point values are

$$\dot{p_1} = -\underset{\sim}{N}c_1^2 \tag{2.74}$$

$$\dot{c_1} = -\underset{\sim}{N}c_1(p_2 + p_3 - p_1) \tag{2.75}$$

which can be solved exactly to obtain

$$p_1(t) = p_2 + p_3 - 2\sqrt{p_2 p_3}tanh(2\sqrt{p_2 p_3}\underset{\sim}{N}(t - t_o)) \tag{2.76}$$

$$c_1(t) = \pm 2\sqrt{p_2 p_3}sech(2\sqrt{p_2 p_3}\underset{\sim}{N}(t - t_o)) \tag{2.77}$$

These are the Bianchi II solutions written in these variables. The p_1 transitions between one Kasner solution at $t = -\infty$ and another at $t = +\infty$.

$$p_1(-\infty) = p_2 + p_3 + 2\sqrt{p_2 p_3} = (\sqrt{p_2} + \sqrt{p_3})^2 \tag{2.78}$$

$$p_1(+\infty) = p_2 + p_3 - 2\sqrt{p_2 p_3} = (\sqrt{p_2} - \sqrt{p_3})^2 \tag{2.79}$$

2.7.1 The u-map

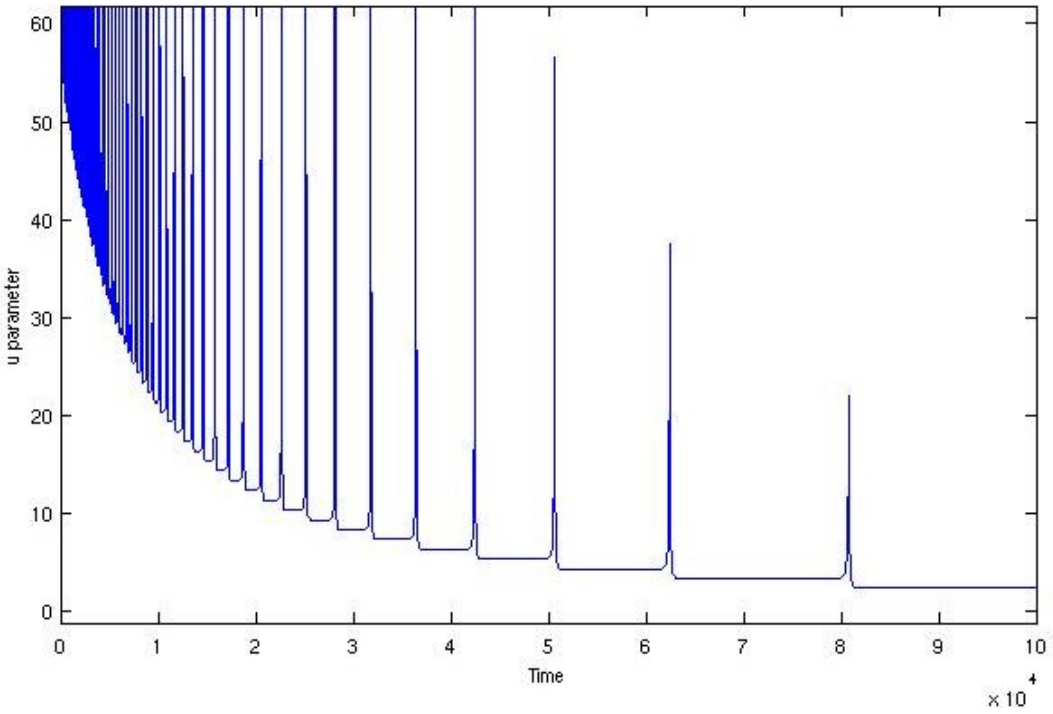

Figure 2.3. Long term u-map showing transitions between Kasner phases over time - the u parameter steps down by 1 at each transition

The transitions described in the previous section can be used to derive the so called 'u-map' relating initial and final states of these processes. This map has often been observed in numerical simulations [25] [14] and its analytic basis examined [27]. In this process we begin with a perturbation of a Kasner state described by the parameter u_i. To recover u from 2.65 we take the ratio of the largest to second largest exponents, $u_i = p_1/p_2$. The largest exponent at the end of the transition is p_2 and from 2.78 we see that if $u_i > 2$ then the second largest is

p_1, if $u_i < 2$ the second largest is p_3. Therefore we find that the Kasner parameter defining the final state u_f is given by

$$u_f = \begin{cases} u_i - 1 & \text{if } u_i \geq 2 \\ (u_i - 1)^{-1} & \text{if } u_i < 2 \end{cases} \tag{2.80}$$

Once this transition is complete, we can then relabel the p_i so that they are again in descending order and repeat the process. Thereby we see a discrete structure emerge from our equations, as we set $u_n = u_i$ and $u_{n+1} = u_f$. Although for generic initial values the orbit of u visits most of the real line, there are certain preserved structures. As an example, $u = \{1 + \sqrt{2}, \sqrt{2}\}$ is a 2-cycle point of the map, and in fact cycles of all lengths exist [26], given by the cases when u is a quadratic irrational [2]. By construction the map leaves $\mathbf{Q}$ invariant, and should it ever encounter $\mathbf{Z}$ it should in theory end at ∞. However, these points are highly unstable and any perturbation around them will obviously evolve away from them. Indeed for any $\epsilon > 0$ we find that if $u_i = n + \epsilon$ for some $n \in \mathbf{Z}$ then on its orbit under this map, u will visit $1/\epsilon$. However, since our map was obtained by making approximation, we cannot expect it to hold exactly in any physical system, and hence no transition can be expected to take us to $u \to \infty$, which would correspond to $p_i = \{1, 0, 0\}$.

The map is also an example of the high degree of chaos in our system - a point in space might be described by $u_n = 2 + \epsilon$ where $\epsilon > 0$ $u_{n+1} = 1 + \epsilon$. However a nearby point in an inhomogeneous space could be described by $u_n = 2 - \epsilon$ in which case $u_{n+1} = 1/(1 - \epsilon)$.

In figure 2.3 we see a long term evolution of the u parameter. Note that it takes on stable values for large periods of time and then undergoes a transition, the points where the parameter appears to peak upwards. This is the u-map for the system simulated above in 2.1.

In the figure2.3 we see only the first type of transition, in which the value of u is reduced by one. To observe the second type of transition we must see a situation in which p_1 goes from being the largest eigenvalue to the smallest. This is realized in the following simulation

[2] This corresponds to $u = q_1 + \sqrt{q_2}$ where $\sqrt{q_2}$ is not rational

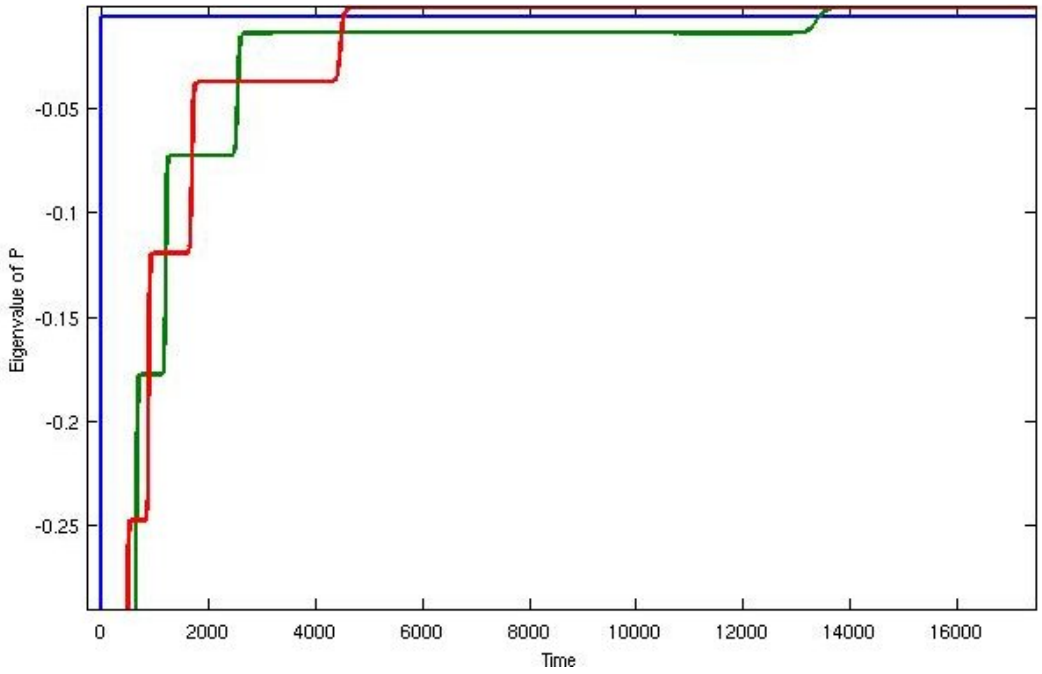

Figure 2.4. Evolution of in which highest eigenvalue of P crosses both others

In simulation 2.5 we see the corresponding evolution for the u parameter:

The labeled point on this simulation is at $u = 1.88$ with the preceding value being $u = 1.53$, which agrees with the behavior of the u-map to within 1%.

Further simulations showing this behavior can be seen in appendix A.

2.7.2 Spikes

Seen initially in both numerical simulations of Gowdy and generic space-times, explicit analytical 'spike' solutions have recently been found [28]. In numerical simulations of the full equations there are points in space at which the derivatives of spatial and extrinsic curvature grow to a large value before shrinking again. This would appear at first glance to break the model we propose - a model in which these derivative terms are negligible. However, an analysis of the simulations shows that these spikes do not appear to occur in the neighborhood of the singularity.

On examination of the space-time of [28] we find that the asymptotic behavior of our variables is still such that the assumptions about negligible terms hold - as we move away from the spike points in both time and space the derivative terms

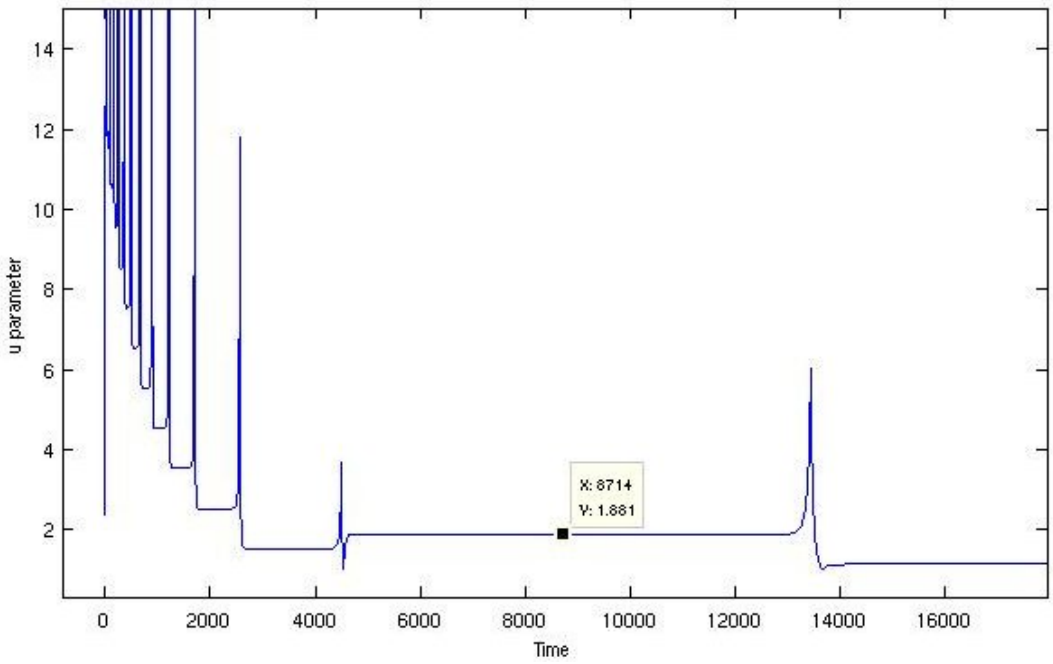

Figure 2.5. Evolution exhibiting both parts of u-map

tend to zero as a result of the asymptotic behavior of the triad. However the question remains - Does our model predict the existence of these spikes?

Surprisingly, the answer is yes. Although the spikes are a *cause* of non negligible derivative terms, they are a *result* of the terms polynomial in curvature, as we will show: Throughout a Taub transition we find that the sign of C_I is preserved. Suppose that we consider all points in space to be described by the dynamics above, then $C = C^0(x^a)$ is a field in space at some time. There may generically exists points X about which C^0 passes through zero. On one side of this point C_I is positive and increasing in magnitude, on the other it is negative and increasing in magnitude. Hence about this point the gradient, $\widetilde{D}_J C_I$ will increase rapidly. These points are precisely the 'spike' points - the spatial derivatives of P and C become large here. In figures 2.6 2.7 we vary the initial eigenvalues of P about a point which is stable. On either side a transition occurs, with C undergoing Taub transitions with *opposite* signs.

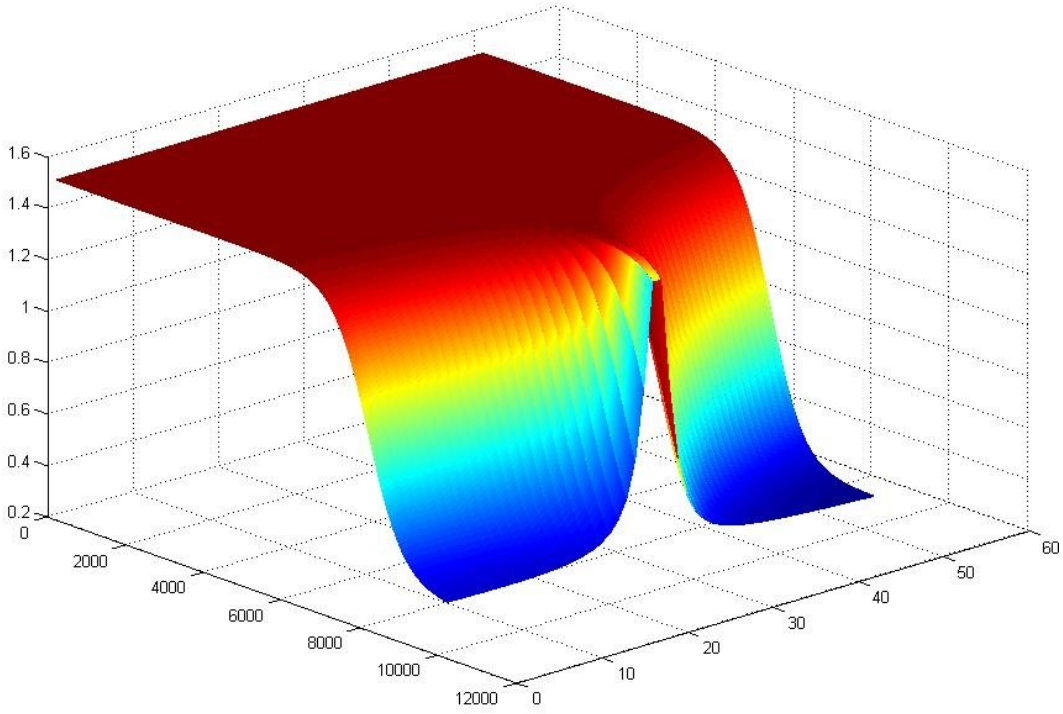

Figure 2.6. Spike in the eigenvalue of P - on either side of the spike point transitions occur but at the point the eigenvalue remains constant

2.7.3 Function Fitting

In the previous sections we found that during a transitional phase described by 2.76 the evolution of C was well approximated by a *sech* function. In performing this analysis we made the approximation that only one of the eigenvalues of C was non-zero during the transition, and hence that only one of the eigenvalues of P was changing. However, a remarkable numerical result that was not shown analytically is that this approximation appears to work away from this point. In fact, it appears that even when all three eigenvalues of C are non-zero, the evolution is well approximated by a sum of these functions.

In 2.8 we see the eigenvalues of C in primary colors (red, green, blue) and a five-point fit by a sum of sech functions in secondary colors (yellow, cyan, magenta). This phenomenon is described in more detail in appendix A.

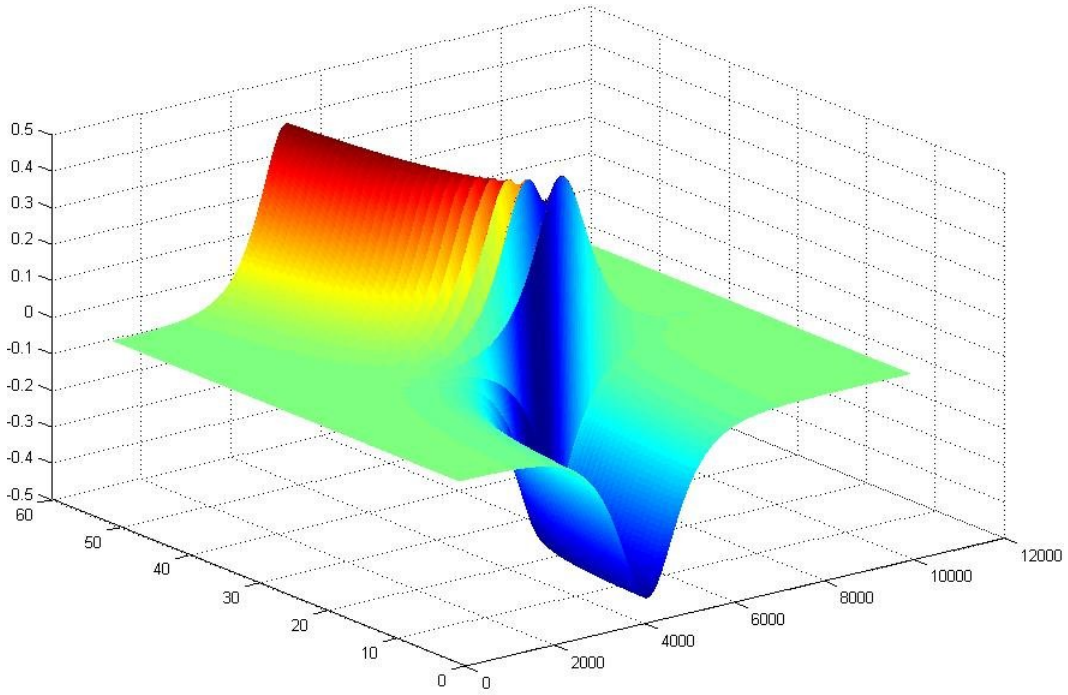

Figure 2.7. Spike in eigenvalue of C - across the spike point large gradients grow

2.8 Conclusion

It has been established in the UEWE framework that by dividing divergent variables by the trace of the extrinsic curvature a set of scale invariant variables can be formed which are well suited to examining the BKL conjecture[25]. This formulation exhibited interesting features such as the Mixmaster dynamics and the u-map. However, this system is not well suited to any quantization procedure based on Hamiltonian systems.

By using density weighted tensors and in particular contractions with a density weighted orthonormal triad instead of division by extrinsic curvature to normalize our variables we obtain a system which is both simple to evolve and well adapted for quantization. In particular, given an initial set of data consisting of an orthonormal triad and extrinsic curvature $(\widetilde{E^a_i}, K^i_a)$ it suffices to form $\widetilde{P_{ij}}$, $\widetilde{C_{ij}}$ and $\widetilde{D_i}$ and consider the system of only this triplet. Once this system has been solved, one can the return to the initial variables and recover their evolution of $\widetilde{E}$ for example from the behavior of the triplet. As such a Hamiltonian analysis of the BKL con-

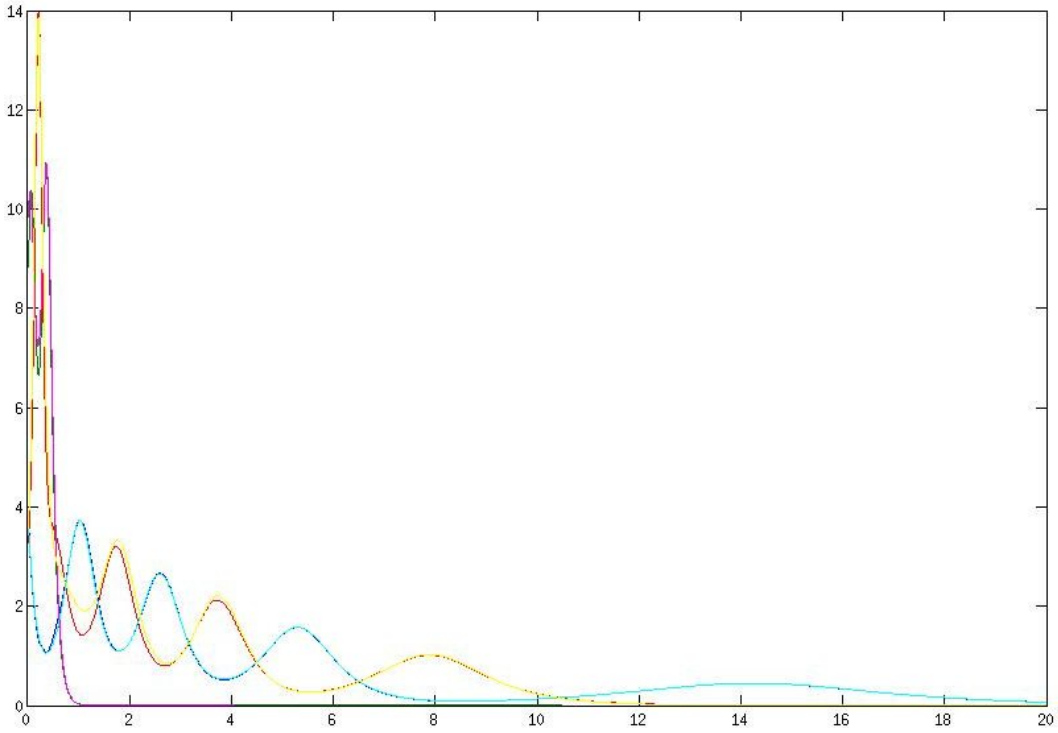

Figure 2.8. Fit of the evolution of the eigenvalues of C by a sum of sech functions

jecture is a valuable tool for probing questions of the generic nature of singularity resolution in LQC. The current status singularity resolution in LQC bears a striking resemblance to that of the big bang singularity. In specific symmetric cases singularity resolution has been shown, but as yet there is not generic singularity resolution theorem. A close analysis of the BKL conjecture could provide a step towards that goal.

Through a detailed examination of the BKL system proposed, both numerically and analytically, we see that there does indeed exist a well defined subspace of the full phase space of GR which exhibits exactly the properties expected by the BKL conjecture. By gauge-fixing our constraints, we do observe the Mixmaster behavior, a series of Bianchi I spacetimes interspersed by Bianchi II transitions and the presence of spikes. We recover the 'u-map' for these transitions, and observe the behavior expected by Andersson and Rendall when a scalar field of large enough magnitude is introduced. Numerical simulations show that these are exactly the features which we expected from the analysis. Furthermore we see a remarkable fit to the equations of motion by a sum of *sech* functions. Since the solutions to the

BKL truncated system allows for the existence of spike solutions, it is important for quantum theories of cosmology to take into account this feature. As these spikes can be found in exact solutions of GR they are not simply an artifact of our truncation, but potentially a physical phenomenon which should be examined more closely. The truncation we have proposed ignores the effect of these spikes upon dynamics and therefore is unlikely to be suited to their analysis.

Chapter 3

LQC Effective Equations and their Implications

3.1 Introduction

Loop quantum gravity is a background independent approach to the quantization of gravity. It is almost a tautology that non-perturbative quantum field theories are not afforded the luxury of a classical background easily obtained by taking the limit $\hbar \to 0$. Therefore it is necessary to address questions about both the 'ultraviolet' sector of the theory - the high energy density limit in which quantum effects are expected to dominate, and the 'infrared' sector - the low energy limit in which we should recover the classical theory.

Loop quantum cosmology [30] [31] [32] [33] (LQC) arises as the application of the principles of loop quantum gravity [34] to cosmological spacetimes. Through the LQC program it has been seen that the effects of quantum Riemannian geometry lead directly to the resolution of big-bang type singularities[35]. Initially this was shown in the flat FRW case with a massless scalar field [36], but has more recently been extended to both the open [37] and closed [38] cases, and further to Bianchi I [39] and II [40] cosmologies and hybrid quantization of Gowdy models [41]. Furthermore it has been shown that LQC may in fact preclude the existence of *all* so-called 'strong' singularities [42] . It is therefore natural to ask what are the physical predictions of a theory which has such welcome mathematical properties.

In loop quantum gravity, the spectrum of the area operator $\widehat{\mathcal{A}}$ is discrete. This yields an area gap Δ^2 with $\Delta = 4\sqrt{3}\pi\gamma$ which is the minimum non-zero eigenvalue of $\widehat{\mathcal{A}}$. Herein γ is the Barbero-Immirzi parameter, which is fixed to be approximately 0.24 from black hole entropy calculations [43] [44]. In the cosmological context, the net effect of this area gap is that the density operator $\hat{\rho}$ is bounded from above, with its upper bound denoted $\rho_{\text{crit}} = \sqrt{3}/32\pi^2\gamma^2 \sim 0.41\rho_{pl}$. Thus we should expect to see quantum geometry effects once the energy density becomes of the order of the planck density ρ_{pl}. In the isotropic sector it is convenient to take the square root of of the area gap to form a 'length gap' λ.

Throughout this chapter we will work with the effective, semi-classical equations. It has been well established that these effective equations closely follow the full quantum dynamics both in the infra-red where as expected we recover a close approximation to general relativity, but also more surprisingly some results coincide in the ultra-violet limit. This has been established in the case of a massless scalar field[45], and a more complete program of exploration of the range of validity of effective equations is in progress [46]. We will also make the assumption that all matter is minimally coupled - there will be no cross terms of matter and curvature variables.

3.2 Classical Theory

The flat ($k = 0$) homogeneous, isotropic sector of cosmology is described by spacetimes whose metric takes the form

$$ds^2 = -N^2dt^2 + a^2(t)(dx^2 + dy^2 + dz^2) \tag{3.1}$$

Where N is the lapse function, and $a(t)$ the scale factor [29]. The gravitation part of the action in this sector is therefore

$$S[N, a] = \frac{1}{8\pi}\int dt \frac{-3a\dot{a}^2}{N} \tag{3.2}$$

[1] We perform a Legendre transform to obtain the canonical conjugate momenta

[1] In defining this action, we are implicitly assuming that spatial integration has been performed on a fiducial cell of size V_0. In doing so, we introduce extra, non-physical structure to our system

$P_{(a)} = 6a\dot{a}, P_{(N)} = 0$, and Hamiltonian

$$\mathcal{H} = \frac{-N}{8\pi}(\frac{P_{(a)}^2}{12a} + a^3\mathcal{H}_m) \tag{3.3}$$

where $\mathcal{H}_m$ is the matter Hamiltonian [2]. Note that the equation of motion for $P_{(N)}$ ensures that this Hamiltonian is constant. At this stage for reasons of simplicity, let us fix the lapse, $N = 1$ and by doing so we recover the evolution of our system with respect to proper time, by taking $\dot{X} = \{X, \mathcal{H}\}$.

In order to correspond with the LQC system which we will later analyze, let us further perform a change of variables

$$\nu = \frac{\epsilon a^3 V_0}{2\pi\gamma} \quad b = -\frac{4\pi\gamma P_{(a)}}{3V_0 a^2} \tag{3.4}$$

whose Poisson bracket is therefore given by $\{b, \nu\} = 2$. $\epsilon = \pm 1$ is a free choice of the system related to the freedom to pick left- or right-handed triads, and without loss of generality we will choose to work in the positive sector. If we further fix $V_0 = 1$ the gravitational part of our Hamiltonian is given as:

$$\mathcal{H}_g = \frac{3\nu b^2}{4\gamma} \tag{3.5}$$

3.3 Effective Quantum Theory

The holonomy corrections due to LQC result in b being replaced by $\frac{sin(\lambda b)}{\lambda}$ and thus the gravitational part of our Hamiltonian is therefore

$$\mathcal{H}_g = -\frac{3\nu}{4\gamma}\frac{sin^2(\lambda b)}{\lambda^2} \tag{3.6}$$

Note that in the small λ limit, this reproduces the classical Hamiltonian. If one were to include all physical constants, it would become apparent that this limit is precisely the $\hbar \to 0$ limit. Although this change appears to closely reproduce the classical system, the domain of b is now compact, as b now takes values in $[0, \frac{\pi}{\lambda}]$.

in order to perform mathematical operations. A great deal of care has been taken both in the classical and quantum theory to ensure that physical results are independent of this extra structure.

[2] This is equivalently the energy density ρ

This arises as a direct consequence of the eigenvalues of ν having discrete values [47].

The equations of motion for the gravitational variables are

$$\dot{\nu} = \frac{3\nu sin(2\lambda b)}{2\gamma\lambda} \tag{3.7}$$

$$\dot{b} = -\frac{3sin^2(\lambda b)}{2\gamma\lambda^2} + 4\pi\gamma\mathcal{H}_m + 4\pi\gamma\nu\frac{\partial\mathcal{H}_m}{\partial\nu} \tag{3.8}$$

From the first equation we obtain the corrected Friedmann equation

$$H^2 = \frac{8\pi\mathcal{H}_m}{3} - \lambda^2\gamma^2(\frac{8\pi\mathcal{H}_m}{3})^2 \tag{3.9}$$

Where H is the Hubble parameter, $\dot{a}/a = \dot{\nu}/3\nu$. This reduces to the classical Friedmann equation on taking $\lambda \to 0$.

By using our Hamiltonian constraint, we can reduce the second equation to

$$\dot{b} = 4\pi\gamma\nu\frac{\partial\mathcal{H}_m}{\partial\nu} \tag{3.10}$$

In our notation, the equation of state for the matter content of the universe is written

$$\mathcal{H}_m \propto \sum_w \nu^{-(1+w)} \tag{3.11}$$

and hence if we exclude so called phantom matter, the parameter b is monotonic non-increasing. If we make the simplification that the matter content can be described as a sum of perfect fluids each with a single equation of state characterized by w_i with density ρ_i, we can further simplify our equations:

$$\dot{b} = -4\pi\gamma\sum_i(1+w_i)\rho_i \tag{3.12}$$

3.3.1 Critical Density

From our Hamiltonian constraint we find that H_m is bounded above. For ν non-vanishing, we find

$$\mathcal{H}_m = \frac{3sin^2(\lambda b)}{4\gamma\lambda^2} \leq \frac{3}{8\pi\gamma^2\lambda^2} \tag{3.13}$$

and hence we know that our matter density is bounded, with its maximum denoted ρ_{crit}. In the classical limit, we again find that we recover GR as this bound is inversely proportional to λ and hence in taking $\lambda \to 0$ we remove the bound. Using $\mathcal{H}_m = \rho_{\text{crit}}$, we are able to write our corrected Friedmann equation 3.9 in a more familiar form[45]:

$$H^2 = \frac{8\pi\rho}{3}(1 - \frac{\rho}{\rho_{\text{crit}}}) = \rho_{\text{crit}} \tag{3.14}$$

The existence of this critical density is in fact a prediction of the raw quantum theory. In the full dynamics of LQC, it has been shown [48] that the density operator has a supremum on the physical Hilbert space. This supremum is precisely the critical density encountered by the effective theory. Thus the effective equations reproduce a key feature of the full dynamics in the deep quantum regime, and one which should be expected to lead to singularity resolution.

The critical density here is about 41% of the Planck density, which upon restoring fundamental constants is given by

$$\rho_{\text{crit}} = 0.41 * \frac{c^5}{G^2\hbar} = 2.11 \times 10^{96} kg\, m^{-3} \tag{3.15}$$

To obtain a sense of proportion, this density is the equivalent to having the entire mass of the Milky Way galaxy within the one thousandth of the classical radius of the electron.

3.3.2 Quantum Bounce

It is immediately apparent from 3.7 that the evolution of the Hubble parameter $H = \frac{\dot{\nu}}{3\nu} = \frac{\dot{a}}{a}$ is significantly altered when b is close to $\frac{\pi}{2\lambda}$. In fact, at this point $\dot{\nu}$ changes sign, and thus contraction of the universe ends and expansion begins.

Here it is clear that the Hubble parameter can only change sign once the energy density reaches the critical density, and that away from this critical density the effects of quantum geometry are small. Thus LQC provides ultraviolet corrections to GR whilst maintaining infrared physics. Due to these corrections, dynamical

trajectories avoid the cosmological singularity, which is in the past of any expanding branch (or future of any contracting branch) in classical GR and form a quantum bridge between the two branches throughout which physics remains finite and deterministic.

In order to establish that $\nu = 0$ is not achievable by our system, consider $Y = ln(\nu)$ then

$$\dot{Y} = \frac{\dot{\nu}}{\nu} = 3H = \frac{3sin(2\lambda b)}{2\gamma\lambda} \tag{3.16}$$

Hence in any finite time, the change in this log volume, is given by

$$\Delta Y = \int dt\dot{Y} = \frac{3}{2\gamma\lambda}\int dtsin(2\lambda b) \tag{3.17}$$

and hence we obtain a bound

$$|\Delta Y| \leq \frac{3}{2\gamma\lambda}\int dt|sin(2\lambda b)| \leq \frac{3\Delta t}{2\gamma\lambda} \tag{3.18}$$

since *sin* is bounded by 1. Therefore for the volume to go to zero, we would require $Y \to -\infty$ which is not possible in a finite amount of proper time. This result establishes that no trajectory on which the volume ν is non-zero can achieve zero volume.

Since ν is either always positive or always negative, and physics does not change between these choices, we are justified in choosing $\nu > 0$ on all our solutions and ignoring the corresponding $\nu < 0$ states.

3.3.3 Inflation

The nature of slow-roll inflation in cosmology in general, and LQC in particular will be discussed in detail in the following chapter. There we shall restrict ourselves to considering the effects of a scalar field. However, the existence of inflation under generic conditions is another feature of LQC [49]. The term inflation relates to a period in the expansion of the universe in which the scale factor is accelerating, $\ddot{a} > 0$. Since $\nu \sim a^3$ we find:

$$\frac{\ddot{a}}{a} = \frac{\ddot{\nu}}{3\nu} - \frac{2\dot{\nu}^2}{9\nu^2} \tag{3.19}$$

$$= \frac{sin^2(2\lambda b)}{4\lambda^2\gamma^2} + \frac{\dot{b}cos(2\lambda b)}{\gamma} \tag{3.20}$$

Upon applying some trigonometric identities, and re-writing our equation in terms of the matter density ρ we find:

$$\frac{\ddot{a}}{a} = \frac{8\pi\rho}{3}\sqrt{1 - \frac{\rho}{\rho_{\text{crit}}}} + 4\pi\nu\frac{\partial\mathcal{H}_m}{\partial\nu}(1 - \frac{2\rho}{\rho_{\text{crit}}}) \tag{3.21}$$

On assuming that the only matter present is a mixture of perfect fluids with equation of state $p_i = w_i\rho_i$, we can again further simplify

$$\frac{\ddot{a}}{a} = \frac{8\pi\rho}{3}\sqrt{1 - \frac{\rho}{\rho_{\text{crit}}}} - 4\pi(\sum_i(1 + w_i)\rho_i)(1 - \frac{2\rho}{\rho_{\text{crit}}}) \tag{3.22}$$

In the low density, single field limit ($\rho << \rho_{\text{crit}}$) we recover the familiar Raychaudhuri equation:

$$\frac{\ddot{a}}{a} = -\frac{4\pi\rho}{3}(1 + 3w) \tag{3.23}$$

3.3.4 Superinflation

Superinflation refers to a phase in the evolution of the universe in which the Hubble parameter is increasing over time ($\dot{H} > 0$). In any cyclic or bouncing cosmology there must necessarily exist a period of superinflation, since in all contracting branches $H < 0$ and in expanding branches $H > 0$. This is indeed observed in solutions to LQC [50] However, in GR this is achievable only through the introduction of 'exotic' matter, such as dilaton fields. In the case of normal matter, the Hubble parameter is monotonically decreasing (or increasing) on expanding (contracting) branches.

Note that superinflation necessarily implies inflation. Since $H = \dot{a}/a$ we therefore find:

$$\dot{H} = \frac{\ddot{a}}{a} - \frac{\dot{a}^2}{a^2} = \frac{\ddot{a}}{a} - H^2 \tag{3.24}$$

and therefore for $\dot{H} > 0$ we necessarily require $\ddot{a}/a > H^2 \geq 0$.

This period of superinflation exists when the energy density is greater than half of the critical density. From 3.14 we establish that the Hubble parameter H evolves via

$$\dot{H} = \frac{\dot{b}cos(2\lambda b)}{\gamma} = \frac{\dot{b}}{\gamma}(1 - 2sin^2(\lambda b) \tag{3.25}$$

$$= \frac{\dot{b}}{\gamma}(1 - \frac{2\rho}{\rho_{\text{crit}}}) \tag{3.26}$$

Since b is monotonic non-increasing $\dot{b} \leq 0$ and hence in this regime we see superinflation. It is a striking signature of LQC that given minimally coupled, non-phantom matter, the universe will superinflate whilst $\rho > \rho_{\text{crit}}/2$ *regardless of the form of the matter itself.*

3.3.5 Bounded Hubble Parameter

By considering the conditions for the beginning and end of this superinflationary phase we observe another feature of LQC: The Hubble parameter is bounded and achieves its bounds. In particular, we know that at the onset and end of superinflation $\dot{H} = 0$. The above conditions yield $\rho = \rho_{\text{crit}}/2$ and so from 3.14 it is obvious that we are still not in a region where LQC agrees with GR.

Further from these conditions we find at the end of superinflation

$$H = \pm\sqrt{\frac{2\pi\rho_{\text{crit}}}{3}} \approx \pm 0.93 \tag{3.27}$$

Since b is monotonic non-increasing, the matter density of each trajectory achieve each of these exactly once, that is *every* contracting solution passes through $H = -0.93$, at which point superinflation begins and persists through the bounce where $H = 0$ and then superinflates to the point $H = 0.93$, before the Hubble parameter starts to fall again.

The equation of state for the matter content will further constrain $\dot{H}$ as follows:

$$\dot{H} = \frac{\dot{b}}{\gamma}(1 - \frac{2\rho}{\rho_{\rm crit}}) \tag{3.28}$$

$$= -4\pi(1+w)\rho(1 - \frac{2\rho}{\rho_{\rm crit}}) \tag{3.29}$$

Since the density is bounded above by the critical density, $\dot{H}$ is therefore bounded between $\pm 4\pi(1+w)\rho_{\rm crit}$.

Note that the above, however, assumes a single field with fixed equation of state. A more complicated system, such as that of a scalar field in a potential, may violate this constraint. In this case we should vary separately the equation of state and the density and maximize each to obtain the bound

$$|\dot{H}| \leq 8\pi\rho_{\rm crit} \approx 10.3 \tag{3.30}$$

Note that this bound is an absolute maximum on the space of all trajectories but is not necessarily achieved on a given trajectory. For a typical evolution of this see figure 3.1.

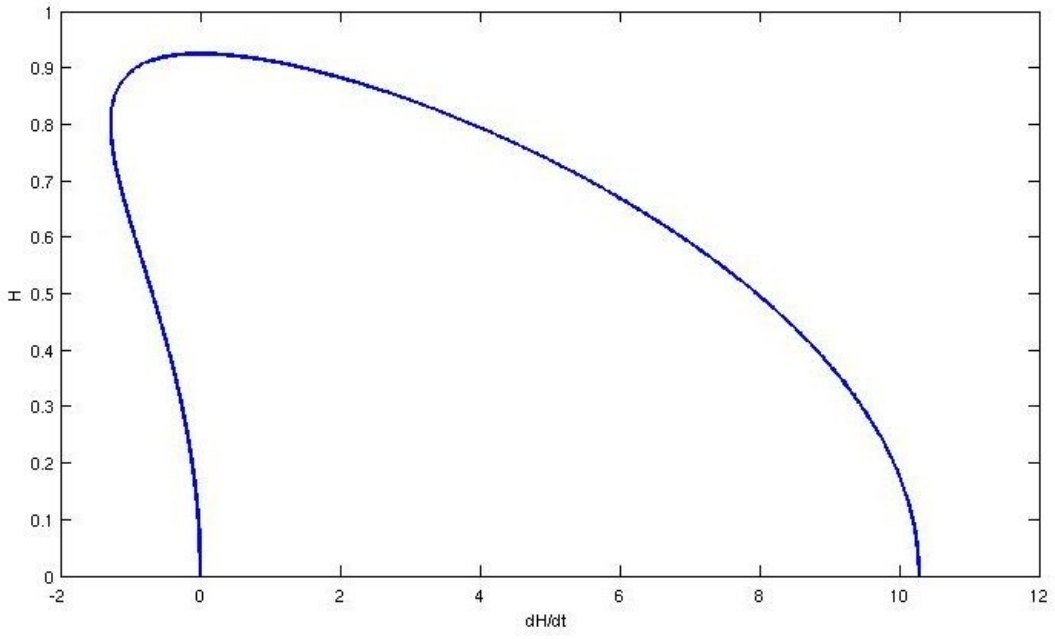

Figure 3.1. Hubble and its time derivative. Time runs counter-clockwise

In figure 3.1 we see the evolution of the Hubble parameter in LQC coupled to a massless scalar field. The right portion of the diagram is entirely quantum effects showing superinflation as here $H > 0$ and $\dot{H} > 0$. The Hubble parameter starts at zero, the bounce point, and increases to its global maximum before descending to follow a path close to that of GR.

From 3.7 and the above, we find that the scalar curvature is bounded above since

$$^4R = 6\dot{H} + H^2 \tag{3.31}$$

Maximizing this independently over $\dot{H}$ and H we find that it is bounded from above:

$$|^4R| < \frac{144\pi\rho_{\text{crit}}}{3} \approx 61.8 \tag{3.32}$$

Note that, as with $\dot{H}$, this is a global maximum, not achieved by all trajectories. In fact it is not attained by any trajectory, as we have separately maximized both H and $\dot{H}$ to obtain it, whereas we know that H achieves it maximum when $\dot{H} = 0$.

3.4 Solutions

We can solve our theory directly in the case of a universe dominated by a single perfect fluid with $w > -1$. We begin from the LQC-Friedmann equations 3.14:

$$(\frac{\dot{\nu}}{3\nu})^2 = \frac{8\pi\beta\nu^{-(1+w)}}{3}(1 - \beta\frac{\nu^{-(1+w)}}{\rho_{\text{crit}}}) \tag{3.33}$$

in which β is chosen such that $\rho = \rho_{\text{crit}}$ at the bounce. We expand our equations to find:

$$\dot{\nu}^2 = \frac{8\pi\beta}{27}\nu^{1-w}(1 - \frac{\beta\nu^{-(1+w)}}{\rho_{\text{crit}}}) \tag{3.34}$$

This can be further rearranged, following the standard method of solving the Friedmann equations in GR to give:

$$\frac{d}{dt}(\nu^{(1+w)/2}) = \frac{2}{1+w}\sqrt{\frac{8\pi\beta}{27}(1 - \frac{\beta\nu^{-(1+w)}}{\rho_{\text{crit}}})} \tag{3.35}$$

Setting $x = \nu^{(1+w)/2}$ and noting that our boundary conditions can be applied by gauge fixing the bounce volume to 1, which in turn sets $\beta = \rho_{\text{crit}}$ we find:

$$x' = \frac{2}{1+w}\sqrt{\frac{8\pi\rho_{\text{crit}}}{27}}\sqrt{1 - x^{-2}} \tag{3.36}$$

Which has solutions:

$$\nu = (1 + \frac{32\pi\rho_{\text{crit}}t^2}{27(1+w)^2})^{\frac{1}{1+w}} \tag{3.37}$$

Where we have chosen $t = 0$ as the bounce point. At late times (t large) as expected this asymptotes to the GR solution in which $\nu \sim t^{\frac{1}{1+w}}$ as the second term in 3.37 dominates. At early times we see corrections, and indeed the bouncing behavior is recovered, with $\nu = 1$ and $\dot{\nu} = 0$ at $t = 0$. Note further that this solution is time symmetric: $t \to -t$ does not affect our system. This property is due to the symmetry of $\mathcal{H}_m$ and in general we do not expect it to persist, particularly when H_m includes interactions. Indeed as will be shown in the following chapter, there can be a great deal of asymmetry in the contracting and expanding branches due to the *phase* of matter at the bounce.

In figure 3.2 we see the evolution of solutions with varying equation of state. The red line depicts a free scalar field ($w = 1$), the green radiation ($w = 1/3$) and the blue dust ($w = 0$)

These solutions clearly exhibit the properties described in section3.3. At large, negative t the solution closely approximates that of GR on an contracting branch. As the density increases, we see that there is inflation when

$$t \in [-\frac{1}{\sqrt{2\pi\rho_{\text{crit}}(1 + 4w + 3w^2)}}\,,\ \frac{1}{\sqrt{2\pi\rho_{\text{crit}}(1 + 4w + 3w^2)}}] \tag{3.38}$$

This period includes super-inflation when

$$t \in [-\frac{1}{\sqrt{6\pi\rho_{\text{crit}}}(1+w)}\,,\ \frac{1}{\sqrt{6\pi\rho_{\text{crit}}}(1+w)}] \tag{3.39}$$

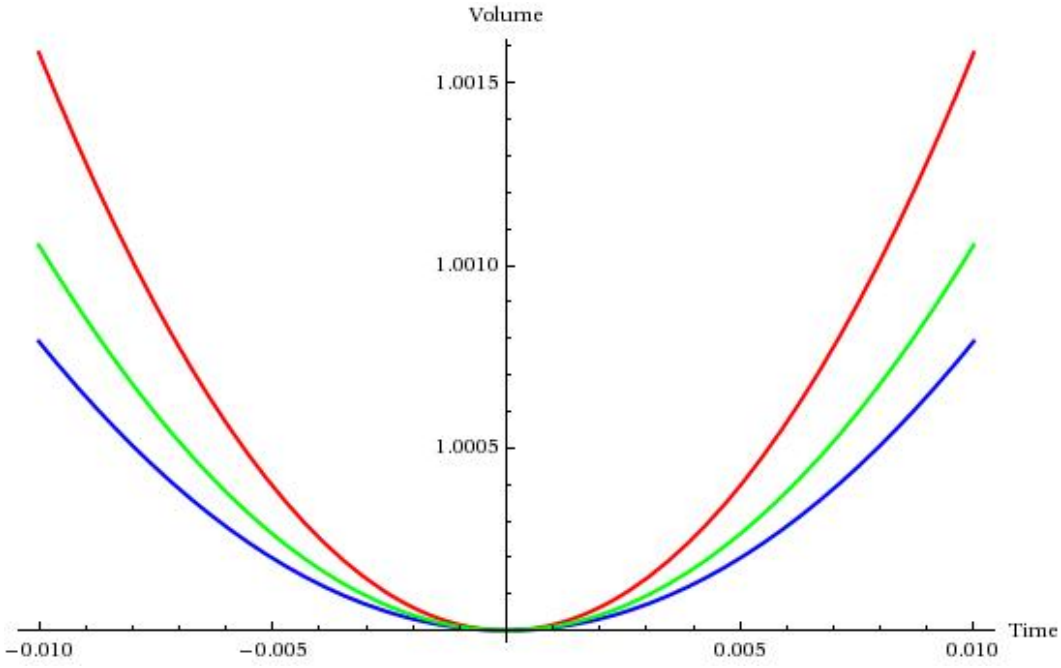

Figure 3.2. Volume evolution for varying matter types

In figure 3.3 we see the evolution of the Hubble parameter for the cases above. We see a period of superinflation in each, which ends at the universe point of the Hubble achieving its maximum. Similarly in figure 3.4 we see the rate of acceleration for the matter types, all of which exhibit inflation for a period.

Of relevant physical interest particulary in forming questions of observables would be questions of how much superinflation or inflation we observe. By taking the ratio of the volumes at the end of superinflation (ν_{es}) and at the bounce (ν_b) we find:

$$\frac{\nu_{es}}{\nu_b} = (2+w)^{\frac{1}{1+w}} \tag{3.40}$$

Remarkably, this factor is entirely *independent* of the critical density, it is simply a function of the equation of state. Similarly one can calculate the amount of inflation with the volume at the end of inflation denoted ν_{ei}:

$$\frac{\nu_{ei}}{\nu_b} = (1 + \frac{3(1+w)^2}{1+4w+3w^2})^{\frac{1}{1+w}} \tag{3.41}$$

Similarly it is possible to view the maxima of the rate of change of the Hubble

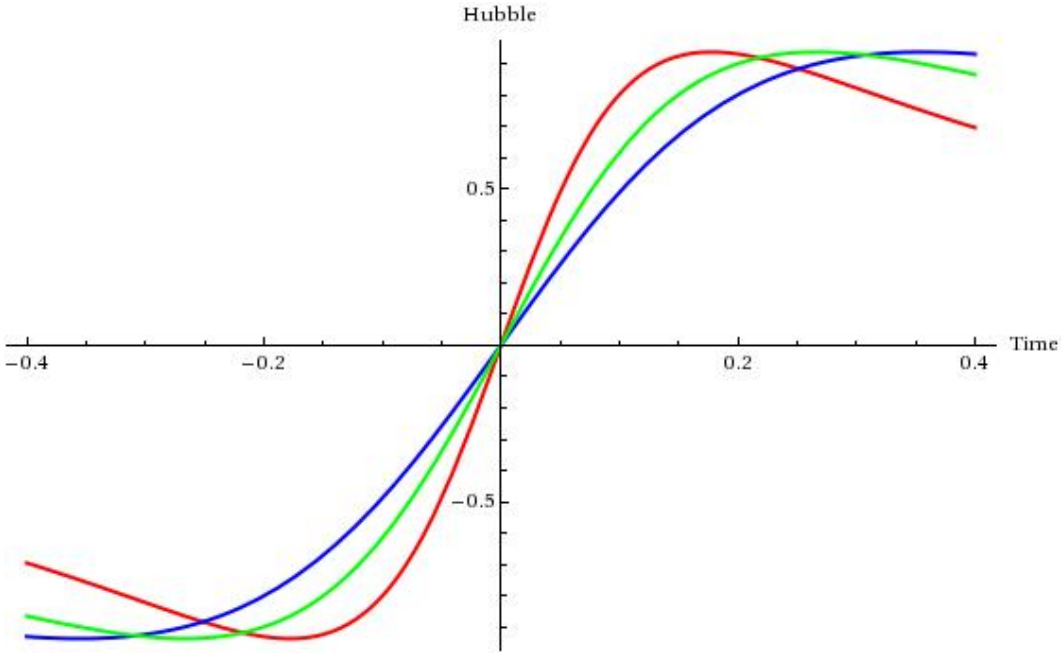

Figure 3.3. Hubble evolution for varying matter types

parameter, given the profile of the solution in terms of H and $\dot{H}$, which is illustrated for the cases above in 3.5.

The bounded nature of H and $\dot{H}$ leads to the scalar curvature, R being bounded. This is plotted in figure 3.6.

3.5 Discussion

The application of the principles of Loop Quantum Gravity to the cosmological sector yields a theory, LQC, which appears to exhibit every aesthetic quality that one could have hoped for: In the cases so far studied in detail, semi-classical solutions at late times both match GR in the infrared limit and receive quantum corrections in the ultraviolet which ultimately lead to the resolution of the big bang singularity. All physically interesting quantities evolve in a deterministic, non-singular manner. On top of all this, LQC exhibits, at least in specific cases a most fortuitous property that appears highly unlikely: There exists a well defined semi-classical set of effective equations which closely match the expectation values of the related quantum evolution of a solution which is semi-classical at late times

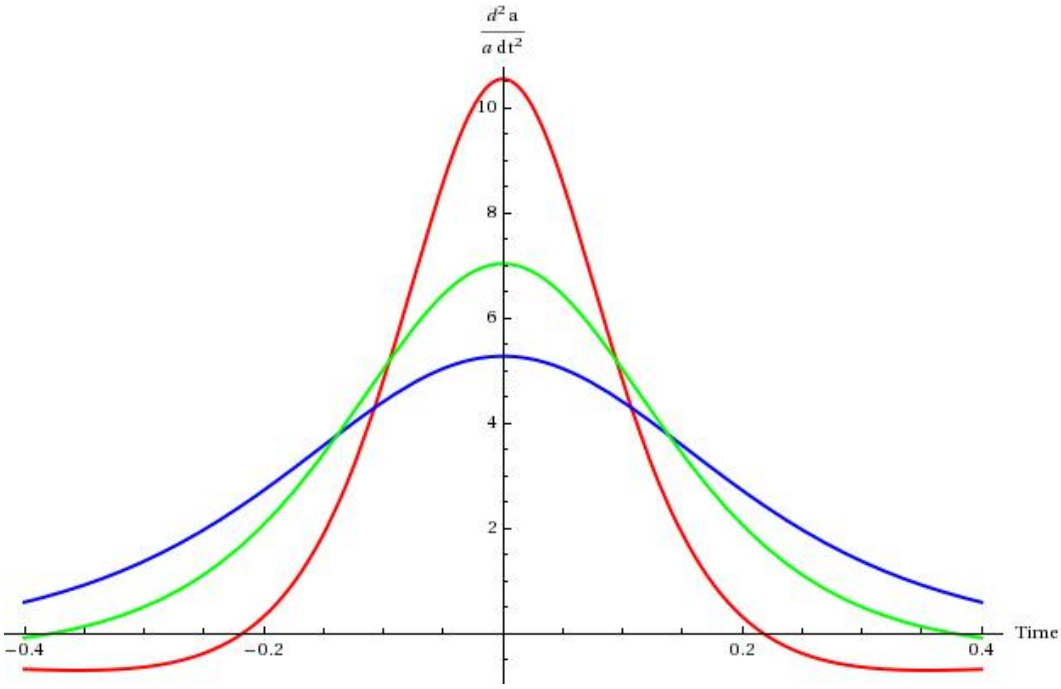

Figure 3.4. Acceleration for varying matter types

throughout the entire evolution. Before performing the analysis, one could not have predicted this with any degree of confidence. The quantum state which is semi-classical at late times could have evolved back into a solution which had a very large dispersion, rendering a classical interpretation of the quantum state meaningless in the planck regime.

Since the effective equations do appear globally effective, it is natural that we should exploit this fortuitous result. In examining these effective equations in a naive fashion, that is without close reference to their origin, we see that they exhibit certain very welcome physical predictions - providing bounds on geometric quantities such as the scalar curvature and Hubble parameter independently of the matter content. We find a Hamiltonian system which is susceptible to standard numerical techniques for solution, and easily coupled to most matter Hamiltonians.

As has been pointed out, it remains to be seen whether such fortune is borne out by examination of more complicated systems, indeed it seems likely that some of the results relating to the effective equations will be altered by a close analysis of more complicated systems.

As an example, the area gap exhibited in the loop quantization of the FRW

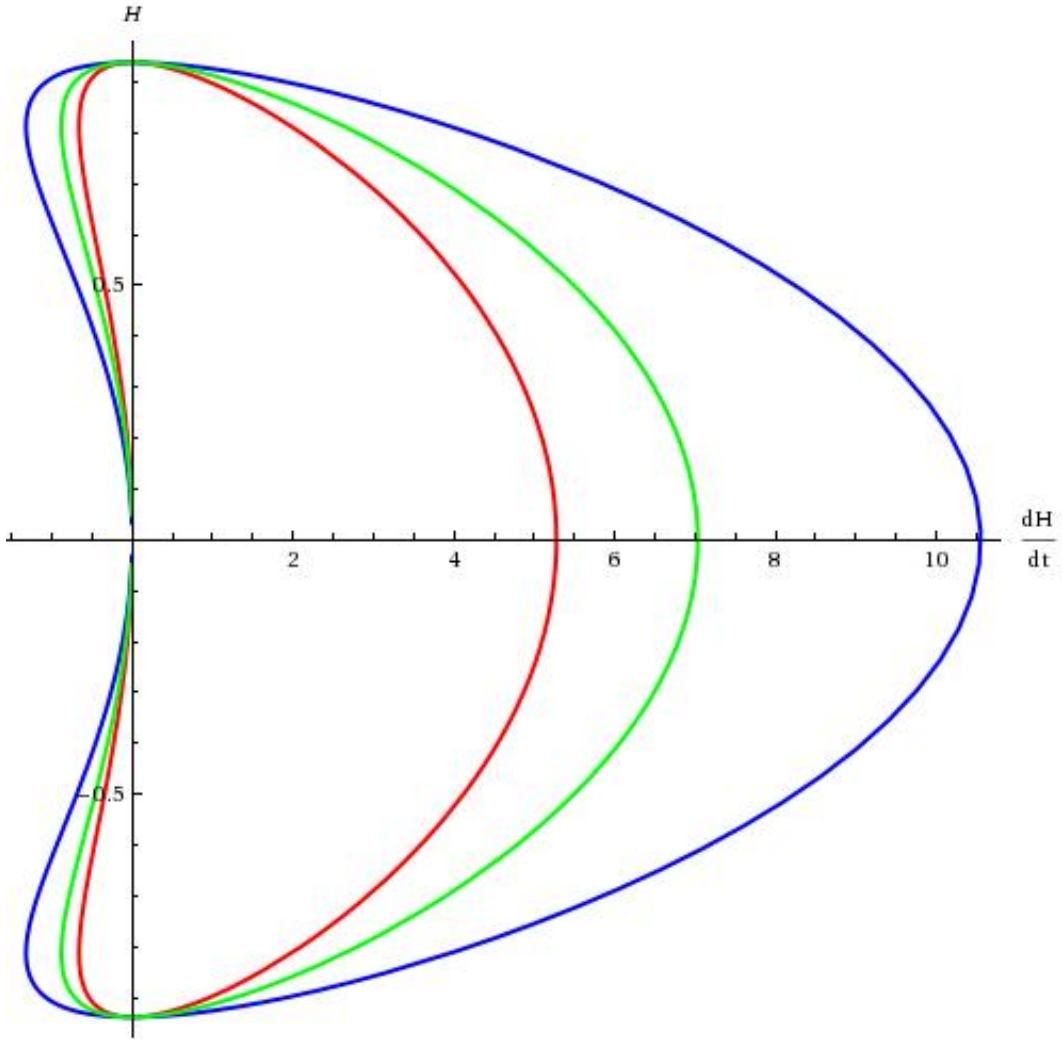

Figure 3.5. Hubble profile for varying matter types - Time runs counter-clockwise from the origin. Here we see for each matter type the universe begins at a large volume which is slowly contracting, the Hubble parameter achieves its lower bound then superinflation begins. The universe superinflates through a quantum bounce (crossing the x axis here) to the maximum of the Hubble parameter and then expansion slows and the universe becomes large again and slowly expanding.

models is half of the supremum of the area operator in Loop Quantum Gravity. [3] Indeed the numerical value of the area gap could change with more input from the full theory on how the area operator is to be formed in the symmetry reduced case. Therefore some overall details will likely change, however it seems reasonable

[3]This is due to an assumption of isotropy that an edge incident on a plaquette must be matched by an exiting edge of same spin and parallel to the incident edge - a condition not required in anisotropic spacetimes - see [51].

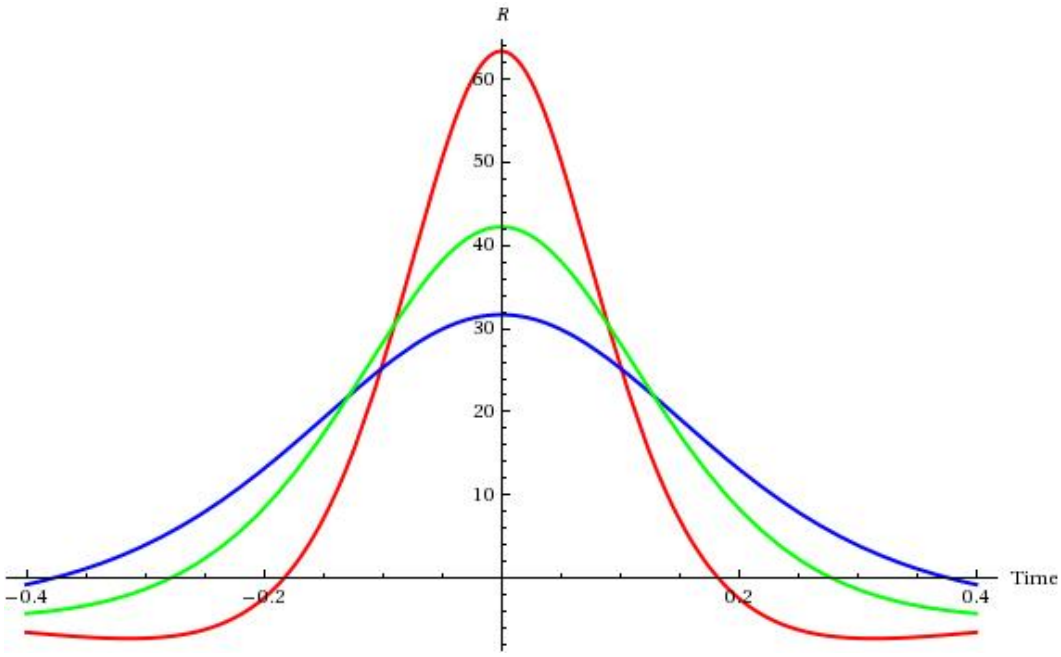

Figure 3.6. Scalar curvature for varying matter types

to expect many of the qualitative features to remain - in particular the existence of bounds on physically relevant quantities.

Chapter 4

Inflation in Loop Quantum Cosmology

4.1 Introduction

Inflation provides an elegant explanation for structure formation in the early universe and has recently enjoyed a great deal of success in this area. Given a sufficiently long period of slow roll inflation, several problems such as those of cosmological horizons and the absence of magnetic monopoles are solved. However, it is argued that achieving this period of inflation requires a great deal of fine tuning. Indeed it was recently stated by Gibbons and Turok [52] that the probability of observing a period of N efolds of inflation, an 'efold' being the increase of the scale factor by a factor of e, is suppressed by a factor of $exp(-3N)$. Since it is typically accepted that at least 68 e-folds would be required to answer the problems above, a heavy burden is placed upon any theoretical framework to explain this apparent fine tuning. It is therefore of key interest to understand if LQC can address this issue. [1]

The basic ideas of inflationary cosmology have been around since the 1970s [54] when it was discovered that a scalar field can be used to model a cosmological constant or 'vacuum energy' - an energy density associated with otherwise empty space. The premise was that this scalar field could fuel a deSitter phase during

[1] This chapter follows the work of the author in [53].

which the universe would undergo an exponential expansion and then a phase transition of the field would end this period. This model was highly unrealistic as it was shown that it results in a highly inhomogeneous universe [55].

A more realistic model was put forward by Starobinsky [56] at the end of the decade, and was the first to predict the now familiar anisotropy of the cosmic microwave background [58]. This model suffered from the 'graceful exit' problem, that different 'bubble' universes would form and collisions between the walls of these bubbles would lead to inhomogeneities.

The modern inflationary model came about in 1981 when Albrecht and Steinhardt [57], and separately Linde [59] modeled the inflaton as a scalar field which is subject to a potential. The scalar field begins in some state on a sloping potential and slowly rolls down this, subject to a friction-like term which arises when considering the effects of a non-zero Hubble parameter. Once this field reaches the minimum of its potential it then decays into other forms of matter, ending the process. Proponents of inflation argue, with varying degrees of success, that it solves a range of cosmological issues. Amongst the more compelling arguments are the horizon problem and the issue of monopoles.

On large scales the universe is observed to be both homogeneous and isotropic. Examination of the the CMB has revealed that the temperature distribution varied by less than 0.1%. However, in the absence of an inflationary phase, these regions would be causally disconnected. Therefore it is a challenge to explain how such regions were in an approximate thermal equilibrium [60]. In a cyclic or bouncing scenario, such as LQC, this problem is at least theoretically addressed - distant parts of space were in causal contact in the distant past, before the bounce. This argument is not entirely satisfactory as it remains to be seen whether regions which have the same temperature down to small fluctuations will remain similar through the highly quantum regime in which the bounce occurs. Inflation not only explains the presence of density fluctuations, but also the observed (almost) scale-invariant spectrum [61] [62].

The question of magnetic monopoles also arises as a spacetime which admits monopoles will be dominated by their presence in the early universe [63]. The production of monopoles would outweigh all the other matter present in the universe by an enormous factor, found to be around 10^{12}. Inflation answers this question if

the universe is inflating either during the production of monopoles or thereafter, as the density of monopoles would be greatly diluted. This is the source of the requirement of 68 efolds - enough inflation that we would expect to see less than one monopole in our cosmic horizon.

The concept of inflation in the very early universe raises two fundamental questions which can be addressed by a quantum theory of gravity. The first relates to the number of efolds, in particular when do we begin counting efolds? Since classically the universe began with a big bang, one cannot simply take the number to be the natural logarithm of the ratio of initial and final scale factors, as the initial scale factor is zero. Therefore one must somehow pick an initial point (in terms of time or density or other physical consideration) from which to count the number of efolds.

The second question is to what degree one should trust the dynamics of GR in the early universe. This relates to the first question, as if one is to make predictions about the spectrum of gravitational waves, say, or the CMB from an inflating cosmology, one must be certain that GR is valid in this region. Since, in our models inflation is to happen *before* the physical phenomena whose structure it explains, one cannot argue that this is a test of the validity of GR here, as it is a modification of GR by the introduction of the inflaton field that we posit as an *explanation* of the observed phenomena.

Fortunately LQC provides us with a well defined answer to both of these questions. Since our cosmological solutions now 'bounce' rather than 'bang' we can begin counting efolds from the bounce point itself, as the scale factor is non-zero here. Also, from 3.14 we find that GR holds to an excellent approximation up to 1% of the critical density, and therefore we are justified in accepting the predictions of GR from this point onwards. In the case of inflation, this turns out to be more than sufficient to answer questions about the CMB observations.

4.2 Preliminaries

We will examine the $k = 0$ cosmological models as these are the most interesting from a phenomenological standpoint. Our system will consist of a 2D configuration space of the volume $\nu \sim a^3$ of our space as measured with respect to a fiducial cell,

and a scalar field ϕ which will play the roll of the inflaton. From these we form our 4D phase space of our configuration variables and their conjugate momenta b, p_ϕ. Dynamics on this phase space is governed by a single constraint, the effective Hamiltonian:

$$\mathcal{H} = \frac{p_\phi^2}{4\pi\gamma\nu} - \frac{3\pi\nu}{4}\frac{sin^2(\lambda b)}{\lambda^2} + 2\pi^2\gamma\nu V(\phi) \tag{4.1}$$

$$\Omega = d\phi \wedge dp_\phi + \frac{1}{2}d\nu \wedge db \tag{4.2}$$

Thus we obtain the effective equations of motion for our phase space variables

$$\dot{\nu} = \frac{3\nu}{2\gamma}\frac{sin(2\lambda b)}{\lambda} \tag{4.3}$$

$$\dot{\phi} = \frac{p_\phi}{2\pi\gamma\nu} \tag{4.4}$$

$$\dot{b} = -\frac{p_\phi^2}{\pi\gamma\nu^2} = -4\pi\gamma\dot{\phi}^2 \tag{4.5}$$

$$\dot{p_\phi} = -2\pi\gamma\nu\frac{\partial V}{\partial\phi} \tag{4.6}$$

It is often convenient in cosmology to consider the Hubble parameter, $H = \frac{\dot{\nu}}{3\nu}$. From 4.3 it is apparent that this is given by:

$$H = \frac{1}{2\gamma}\frac{sin(2\lambda b)}{\lambda} \tag{4.7}$$

and hence we can observe that although in GR H is a monotonic parameter, in LQC it is not. This leads us to consider the variable b - the conjugate momentum to volume - to be fundamental as its evolution is monotonic.

4.3 Gauge symmetry under rescaling

The space of solutions $\mathcal{S}$ to our theory admits a further symmetry in the $k = 0$ case - that of rescaling of volume. Consider the transformation on phase space $\Pi : \{\nu, \phi; b, p_\phi\} \to \{\alpha\nu, \phi; b, \alpha p_\phi\}$. This transformation can be thought of as a shrinking of the fiducial cell from which volume is determined. Since the fiducial

cell itself is a purely extraneous structure which we required to allow a Hamiltonian formulation of our theory, it should have no physical manifestation and this is indeed the case. Under the action of Π we find that the dynamics of the inflaton ϕ and the Hubble parameter H, the physical observables of our theory, are invariant. This transformation generates a flow χ on phase space given by

$$\chi = \nu \frac{\partial}{\partial \nu} + p_\phi \frac{\partial}{\partial p_\phi} \tag{4.8}$$

This flow is not a symplectomorphism, since $\mathcal{L}_\chi \Omega = \Omega$, but it does preserve the constraint surface $\mathcal{H} = 0$ since $\mathcal{L}_\chi \mathcal{H} = \mathcal{H}$ and hence can be considered as a choice of gauge on this surface. For reasons of clarity in what follows we will use this gauge freedom to choose the volume of spacetime at the bounce point, to be given by $\nu_b = 1$. [2] We began with a four dimensional phase space on which we had a single constraint, so the constraint surface is three dimensional. Identifying points connected under the Hamiltonian flow - our dynamical trajectories - further reduces us to a two-dimensional space of solutions to our theory. By further identifying physically equivalent solutions under this rescaling by fixing this gauge freedom we are left with 1 dimensional space of *physically distinct* solutions. For convenience lets us characterize these solutions by the value of the scalar field at the bounce point, ϕ_b. Strictly speaking, the quadratic nature of the constraint only fixes p_ϕ up to a choice of sign. Since we are primarily concerned with potentials which are symmetric under $\phi \to -\phi$, the solutions $\phi_b = \phi_0, p_\phi > 0$ and $\phi_b = -\phi_0, p_\phi < 0$ are physically indistinguishable, and hence considering p_ϕ to be positive at the bounce point and ϕ_b to take both positive and negative values we parameterize all solutions to our theory.

4.4 Inflation in LQC

In this section we will investigate the dynamics of inflation in LQC. Throughout this section we will fix the potential to take a quadratic form, $V(\phi) = m^2\phi^2/2$. For agreement with COBE data we will take the mass parameter to be $m = 6 * 10^{-7}$

[2] This gauge freedom should be familiar from considerations in GR, in which the scale factor a has no physical meaning by itself, and hence one fixes a given value a_0 to be, for example, the value today, and hence only terms such as a/a_0 have physical meaning.

in units of the planck mass[60] which corresponds to about $7 \times 10^{12} GeV$. From our equations of motion 4.3...4.6 one can show that the dynamics of the inflaton are governed by the equation:

$$\ddot{\phi} + 3H\dot{\phi} + m^2\phi = 0 \tag{4.9}$$

This equation bears a striking resemblance to that of a damped harmonic oscillator, with damping parameter $\zeta = H/2m$. For this to be a true harmonic oscillator we would require that H be fixed, whereas in our case it is a dynamical variable. In many of the cases of interest, in particular slow roll inflation, H will be approximately constant and so the analogy will loosely hold. However, elsewhere (in particular in superinflation phase) the evolution of H is significant and this approximation will break.

To simplify the analysis of our dynamics we will consider three separate cases labeled by the distribution of energy in the harmonic oscillator at the bounce. Since at the bounce the Hubble parameter H is zero, 4.9 reduces to the equation of a simple harmonic oscillator, with energy ρ_{crit}.

In particular, let us define $f = \frac{\phi_b}{\phi_{max}} = \frac{m\phi_b}{\sqrt{2\rho_{\text{crit}}}}$. Note that f takes values on $[-1, 1]$.

4.4.1 Strong Kinetic Domination ($|f| < 0.1$)

In the kinetic dominated case, the scalar field is close to its minimum at the bounce point and here we will drop terms of higher order than f^2. Since the potential is small during superinflation, corrections to the massless case due to its presence will be small. The amount of time that superinflation lasts, Δt is well approximated by

$$\frac{\Delta H}{\dot{H_{avg}}} \approx \frac{H_{max}}{2\pi\dot{\phi_b^2}} = \frac{H_{max}}{4\pi\rho_{\text{crit}}(1-f^2)} \approx \frac{H_{max}}{4\pi\rho_{\text{crit}}}(1+f^2) \tag{4.10}$$

From the bounce to the end of superinflation $(H, \dot{H})$ goes from $(0, 4\pi\dot{\phi_b}^2)$ to $(H_{max}, 0)$ Hence we can form an estimate of the number of efolds

$$log(N) = \int H dt \approx H_{avg}\Delta t = H_{avg}\frac{H_{max}}{4\pi\rho_{\text{crit}}}(1+f^2) \approx \frac{H_{max}^2}{8\pi\rho_{\text{crit}}}(1+f^2) \tag{4.11}$$

Using the extreme case, in which the potential is zero, this approximation yields an absolute minimum of 1.08 efolds, which is slightly lower than our true lower bound of $2^{\frac{1}{6}} \approx 1.12$. During this time we can also calculate the change in the inflaton:

$$\Delta\phi = \int \dot{\phi} dt \approx \dot{\phi}_{avg}\Delta T = \frac{H_{max}}{2\pi\sqrt{2\rho_{\text{crit}}}}(1+\frac{f^2}{2}) \approx 0.16(1+\frac{f^2}{2}) \tag{4.12}$$

After the superinflation phase there follows a frictional phase in during which the Hubble parameter decreases and we approach the onset of slow-roll inflation. If $\phi > 0$ at the bounce, during this phase we will encounter a turning point, $\dot{\phi} = 0$, when the inflaton achieves its maximum potential and begins to roll back down. At this turn around point, $\dot{H} = 0$ and we can use the hamiltonian constraint to find the Hubble parameter:

$$H_{ta} = \frac{sin(2\lambda b_{ta})}{2\gamma\lambda} = \frac{sin(\lambda b_{ta})}{\gamma\lambda}\sqrt{1-sin^2(\lambda b_{ta})} = \sqrt{\frac{4\pi}{3}}m\phi_{ta}\sqrt{1-\frac{4\pi\lambda^2 m^2\phi_{ta}^2}{3}} \tag{4.13}$$

To understand this phase better, we split it into two parts: The first, from kinetic energy dominance until parity between kinetic and potential energy, and the second from this parity until the turn around point (where kinetic energy is zero).

From the onset of slow roll inflation, the number of efolds can now be approximated since the overdamping of our system yields:

$$\phi(t) \approx \phi_o e^{-\omega t} \tag{4.14}$$

With $\omega = \frac{m^2}{3H_o}$. Therefore we can calculate the number of efolds using the time taken for the inflaton to exit slow roll ($\phi = O(1)$) by:

$$\underset{\sim}{N} \approx 2\pi \left(1 - \frac{\phi_o^2}{\phi_{\max}^2}\right) \phi_o^2 \ln \phi_o \tag{4.15}$$

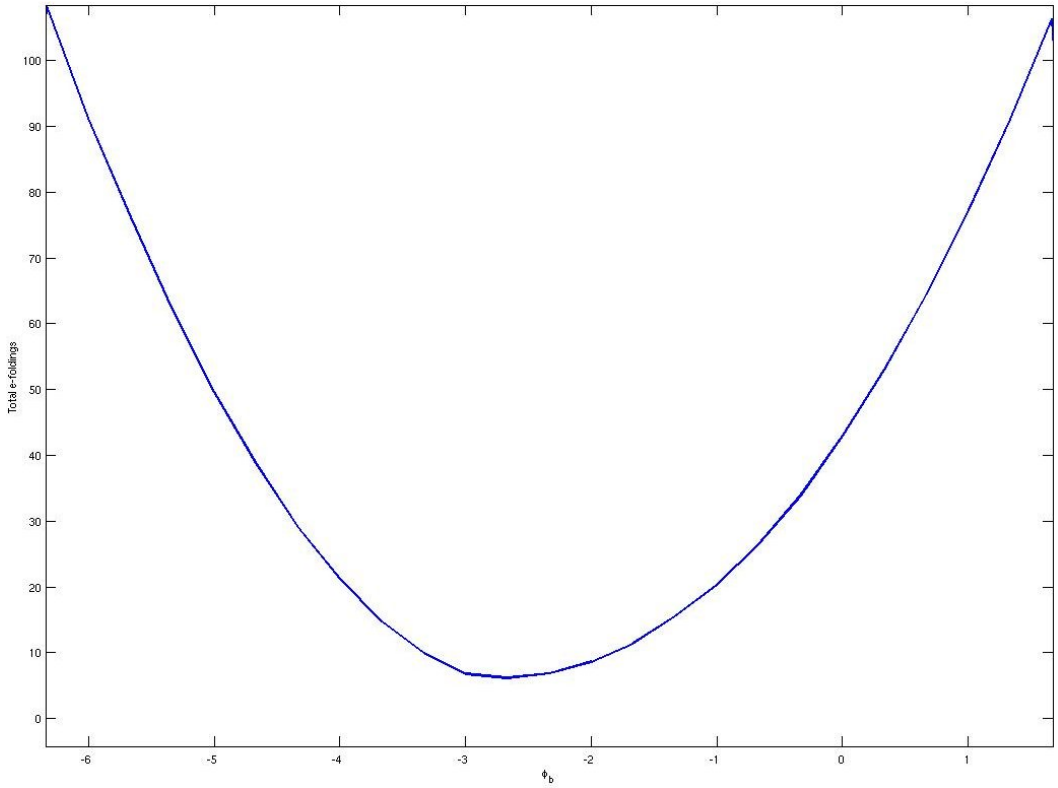

Figure 4.1. Number of efolds vs ϕ_b for small ϕ_b. Note the absolute minimum of about 6 efolds and limited range in which we observe less than 68 efolds.

Taking the further approximation that $\phi_o \approx \phi_b$ since the change in ϕ before this onset is relatively small, we find that the number of efolds of inflation is given by

$$\underset{\sim}{N} \approx 4\pi \frac{\rho_{\text{crit}}}{m^2} f^2(1 - f^2) \ln(|f| \frac{\sqrt{2\rho_{\text{crit}}}}{m}) \tag{4.16}$$

Which gives 68 efolds for $|\phi_b| > 3$ ie $|f| > 2 * 10^{-6}$. From numerical simulations we find 68 efolds for $\phi_b \notin [-5.3, 0.99]$.

This region which does not yield enough inflation is $f \in [-3.5 * 10^{-7}, 6.6 * 10^{-7}]$ which is a very small section of the allowed range. See figure 4.1.

In figure 4.2 we see an example of this extreme kinetic domination case in which there are an insufficient number of e-folds before the slow roll period ends. Here

we observe a rapid superinflationary phase from the bounce point at $t = 0$ followed by a slow roll period in which the number of efolds ($= log(\nu)/3$) increases almost linearly.

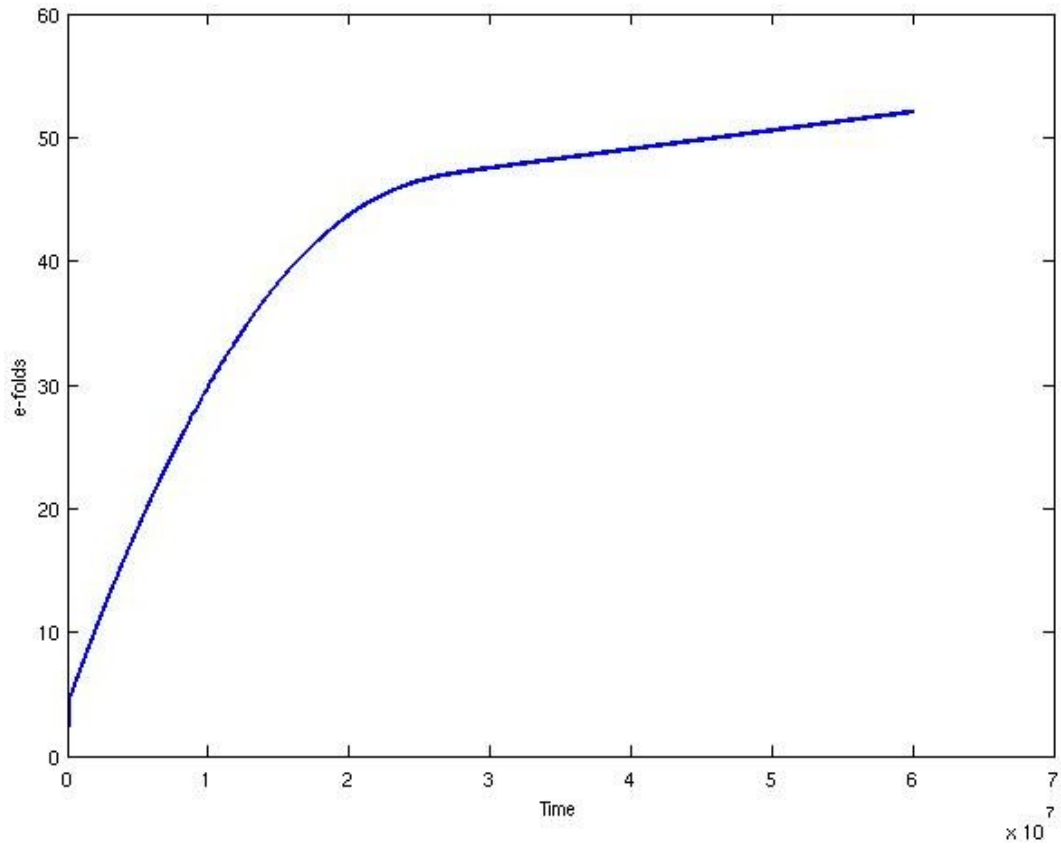

Figure 4.2. E-folds against time for extreme kinetic domination in which we do *not* see 68 efolds.

.

In this simulation we began with $\phi_b = 0.15$ which corresponds to $f = 10^{-7}$ - in the range that indeed we claim will not produce enough e-folds. The time scale here is in planck seconds, and hence we are observing the evolution over the first 10^{-36} seconds after the bounce. The corresponding evolution of the scalar field can be seen in figure 4.3

.

Here we see that the scalar field begins near zero, and rapidly rises up its potential achieving its maximum before returning to slowly roll down its potential. Note that it achieves its minimum at almost the same time as which we observe

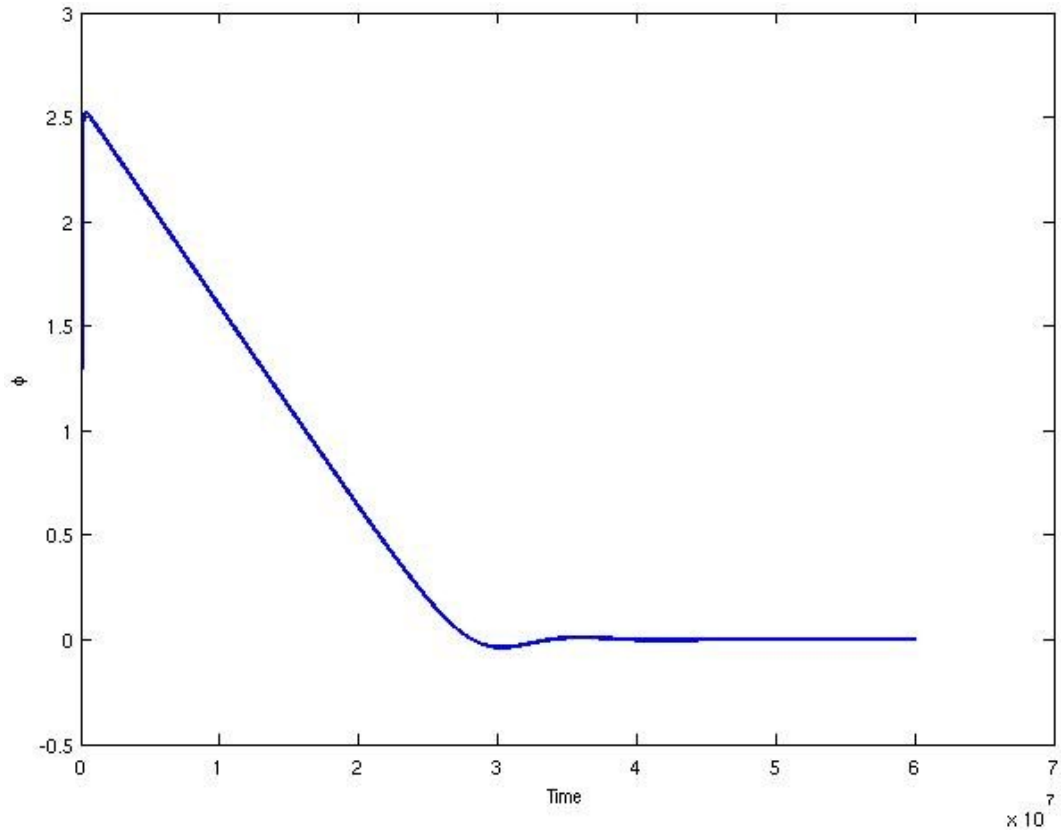

Figure 4.3. Evolution of the scalar field in the extreme kinetic domination case - the field quickly achieves its maximum and begins to slowly roll down.

the linear expansion phase of the number of e-folds to end.

4.4.2 Intermediate Range $0.1 < |f| < 2^{-\frac{1}{2}}$

.

The intermediate range of values is characterized by a short period of super-inflation followed by a long slow roll inflation. When $f < 0.35$ there is a brief non-inflationary period during which the Hubble parameter undergoes a rapid reduction. As f is increased this period becomes shorter, until the point where it ceases to exist at $f \approx 0.35$. The combined period of the short lived superinflation and the inflaton slowing until the onset of slow roll can be seen as the effect of the friction term $3H\dot{\phi}$ in the equation of motion for the inflaton. This friction is coupled to $\dot{\phi}$ and so is essentially removing the kinetic energy of the oscillator. During this phase, the change in the value of the inflaton is negligible as

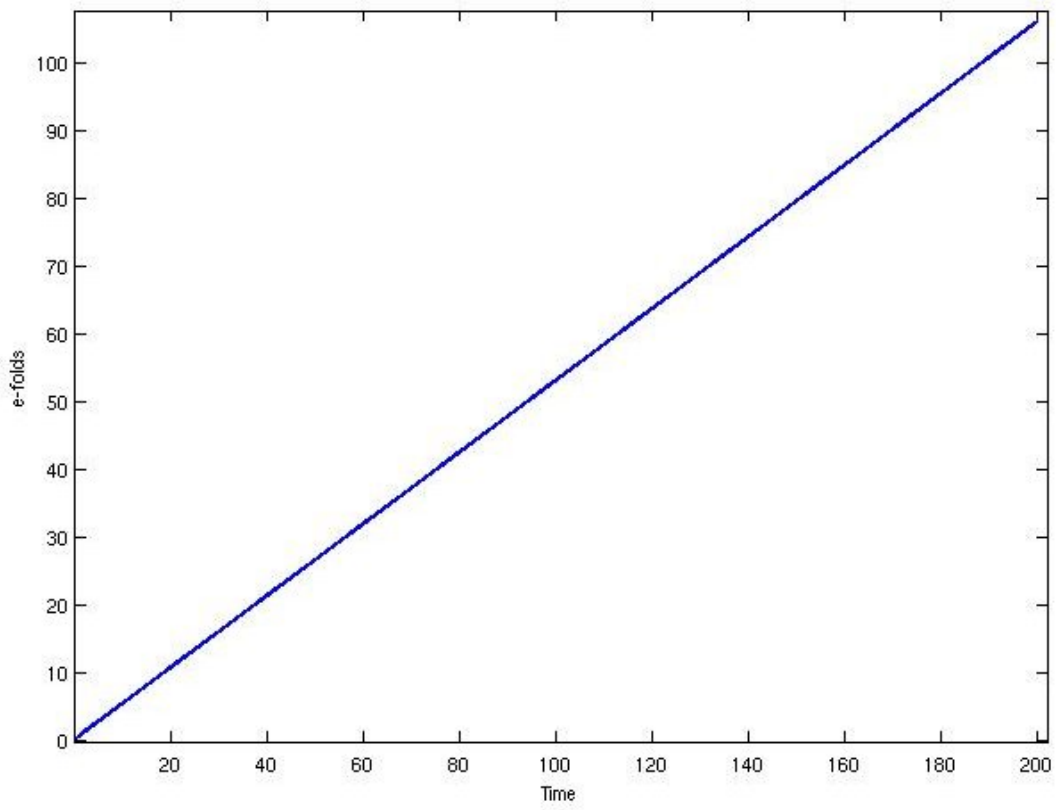

Figure 4.4. E-folds against time for intermediate case, showing a long period of slow roll

$$\frac{\dot{\phi}}{\phi} \approx \frac{\dot{\phi}_b}{\phi_b} = \frac{m\sqrt{1-f^2}}{f} \tag{4.17}$$

which for all f in this range is less than 10^{-5}. Therefore we are justified in making the approximation that the inflaton takes its bounce value at the onset of inflation. We can use this approximation together with 4.15 to show that in this range of f we always get more than 68 efolds.

In figure 4.4 we see that in the intermediate case, slow roll inflation happens very soon after the bounce point. The time scale is again in planck seconds, and so we see that in fact we have achieved enough e-folds incredibly soon after the bounce. In the corresponding evolution of the scalar field, figure 4.5 we see that the inflaton achieves its maximum very soon after the bounce, changing by a negligible amount between the bounce and the turn around point. It then begins its slow roll back down the potential, which will lead to a very large number of e-folds of

slow roll inflation.

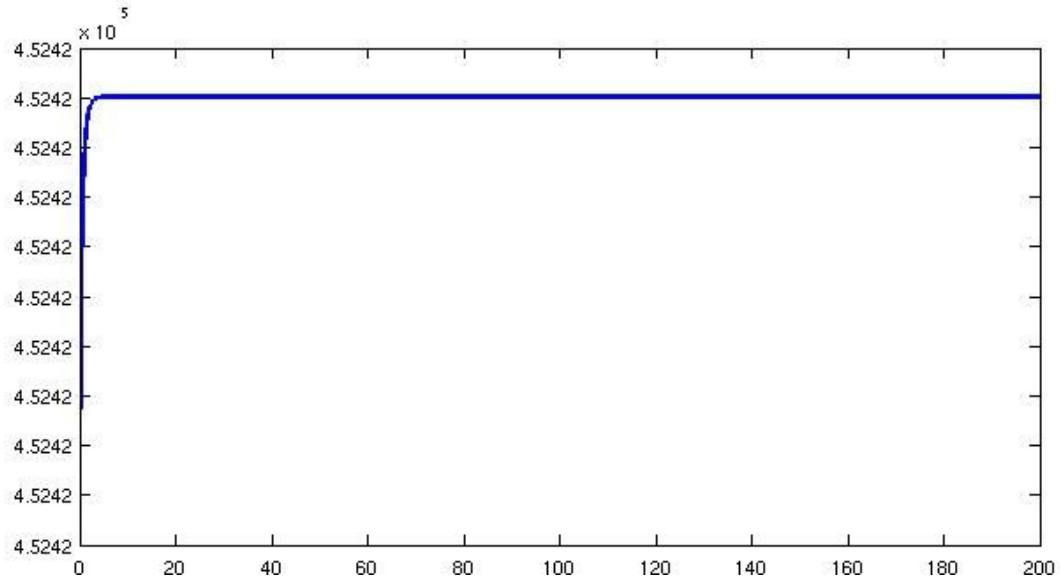

Figure 4.5. Evolution of scalar field for intermediate case - the scalar field reaches its maximum, which is very close to the bounce value, and begins a long period of slow roll.

.

4.4.3 Potential Domination $|f| > 2^{-\frac{1}{2}}$

In the potential dominated case we begin our evolution with energy primarily in the form of potential. Here we see that superinflation can be long lasting and play the main role in the expansion of the universe. If we begin with the scalar field rolling up the potential we see that the turn around must occur during the superinflationary phase, since we begin with $V(\phi) > \rho_{\text{crit}}/2$ and increasing. Therefore at the turnaround, $\dot{\phi} = 0$ the matter density is still above half the critical density, and so still superinflating. We then see that slow roll begins in this region, and hence this phase can be long lived with a high and increasing Hubble parameter. Since superinflation cannot end until the hubble parameter has achieved its maximum value, this will lead to an enormous number of efolds.

.

In figure 4.6 we observe that the Hubble parameter increases rapidly after the bounce point, but does not in fact reach its maximum. Meanwhile the scalar field has reached its maximum value and in fact has begun to slowly roll back down its

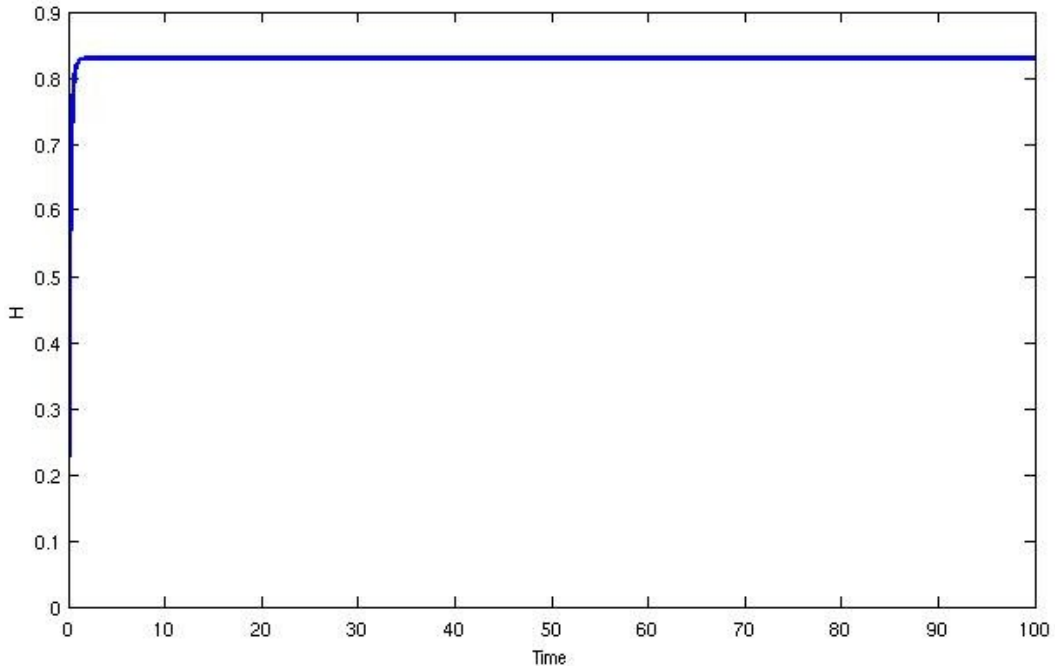

Figure 4.6. Evolution of Hubble parameter in potential dominated case. The Hubble has not yet reached its maximum but is slowly increasing since the scalar field has already begun slow roll. This will result in a large number of efolds.

potential, whilst the Hubble parameter is increasing. This is the origin of the long period of superinflation that we observe in this case.

After super-inflation, the number of efoldings of slow-roll inflation will also be very large. Superinflation ends with the Hubble parameter at its maximum, and due to the massive over-damping from the frictional term, at this point the kinetic energy of the inflaton is low. Hence we exit superinflation with $V(\phi) \approx \frac{\rho_{\text{crit}}}{2}$ and $\dot{\phi}$ small. We can obtain a lower bound for the number of e-foldings for this range of initial values by taking the case where the inflaton begins with energy evenly distributed between kinetic and potential, moving towards its minimum: $\dot{\phi} = -m\phi = \sqrt{2\rho_{\text{crit}}}$.

To gain an estimate of the number of post-superinflation e-folds, we can begin from the condition that superinflation ends, $\rho = \rho_{\text{crit}}/2$. Then the system is again an over-damped harmonic oscillator whose solution is well approximated by 4.14, with initial amplitude $\phi_o = \sqrt{\rho_{\text{crit}}/m}$. Since H is slowly varying over time, in this case from H_{max} to zero, we will approximate its value by $H_{avg} = H_{max}/2$, to obtain

$$\mathcal{N} = \frac{3H_{max}^2}{8m^2} \ln(\frac{\rho_{\rm crit}}{m}) \tag{4.18}$$

Using the values given above, this number is of the order of 10^{13}, greatly in excess of the required 68 e-folds. Despite the huge order of this number, it is not out of keeping with generic inflationary scenarios in GR. Indeed expansions of as many as 10^{130} efolds have been discussed in the literature [60], and as yet there is no observational constraint bounding this number from above.

4.5 Robustness

The results we have obtained so far have all considered the mass of the inflaton to be fixed at $6\times10^{-7}m_p$. This was chosen to be in best agreement with observations, and a quadratic potential was assumed. Since the usual inflationary scenario involves a scalar field oscillating close to the minimum of a potential, this approximation is appropriate. However, in LQC we have established that we are able to explore the entire allowed range of values available to the scalar field subject to the Hamiltonian constraint. Therefore we should consider a more generic set scenarios.

The first consideration is changing the mass of the inflaton. Under a decrease in the mass of the inflaton, the allowed range of initial values of the scalar field increases: Our constraint is that

$$|\phi_b| < \sqrt{2\rho_{\rm crit}}/m \tag{4.19}$$

and hence the range of initial values grows as m^{-1}. In a numerical investigation it becomes apparent that the minimum number of efolds increases as we reduce the mass and the range leading to less than 68 efolds does not grow as quickly as the total range. We find that the range leading to extreme kinetic domination is again smaller as a fraction of the total range. Therefore our results persist under reduction of the mass, even by several orders of magnitude. Under an increase of the mass, we find the the mass of the inflaton must approach $10^{-2}m_p$ before a significant fraction of the solutions do not experience 68 efolds. This is far outside the observational constraints[59] and therefore we are justified in claiming that the results obtained are robust under changing the inflaton mass.

We can further consider a change of the form of the potential. One of the generalizations which agrees with the COBE data is a quartic potential shown in figure 4.7 [60]:

$$V(\phi) = V_0 \pm \frac{m^2\phi^2}{2} + \frac{n\phi^4}{4} \tag{4.20}$$

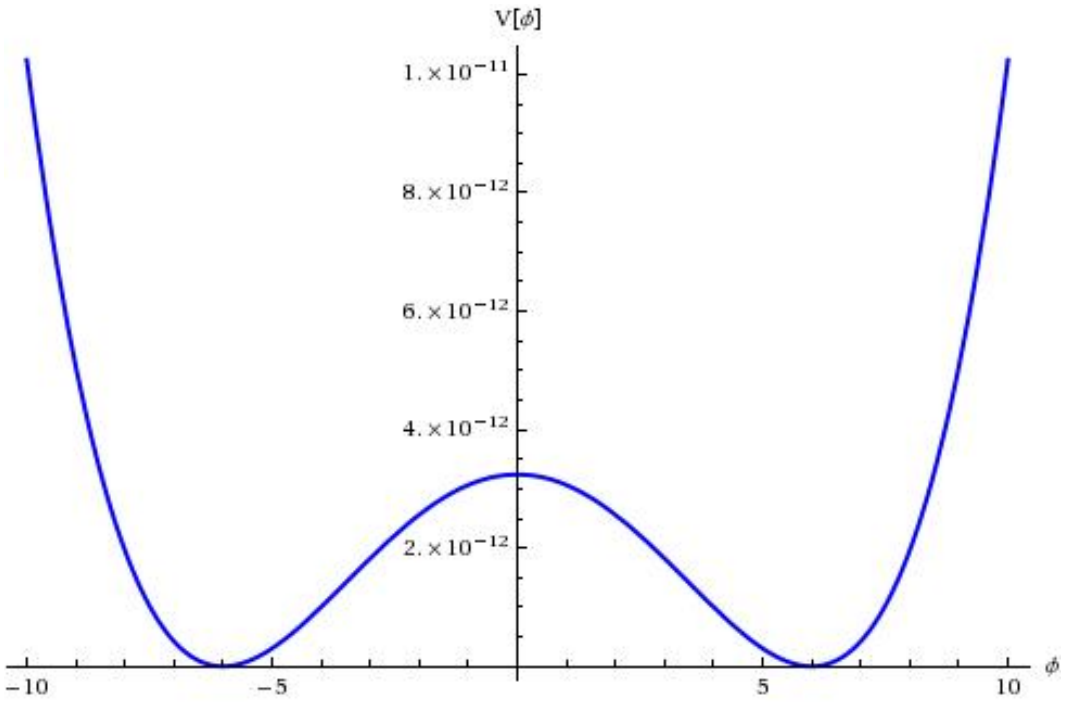

Figure 4.7. The quartic potential with negative sign chosen on quadratic term

.

Where the mass m is restricted as before, and $n \approx 10^{-14}$ for the best fit to the data. To ensure that we have separated the potential from the effects of a cosmological constant, we pick V_0 such that the minimum of this potential is zero. In the case where the sign in front of the quadratic term is positive, this simply implies that $V_0 = 0$. When the sign is negative, this sets $V_0 = m^4/4n$.

If we let $x = \phi + m/\sqrt{n}$ we see that we can then rewrite the potential as

$$V(x) = m^2x^2 - \sqrt{n}mx^3 + \frac{nx^4}{4} \tag{4.21}$$

and hence, as expected, in the large ϕ limit the potential will reproduce that

of a simple $n\phi^4/4$ form. In terms of the dynamics of the scalar field subject to this potential, the effects of the lower order terms are less than 1% for $x > 10$.

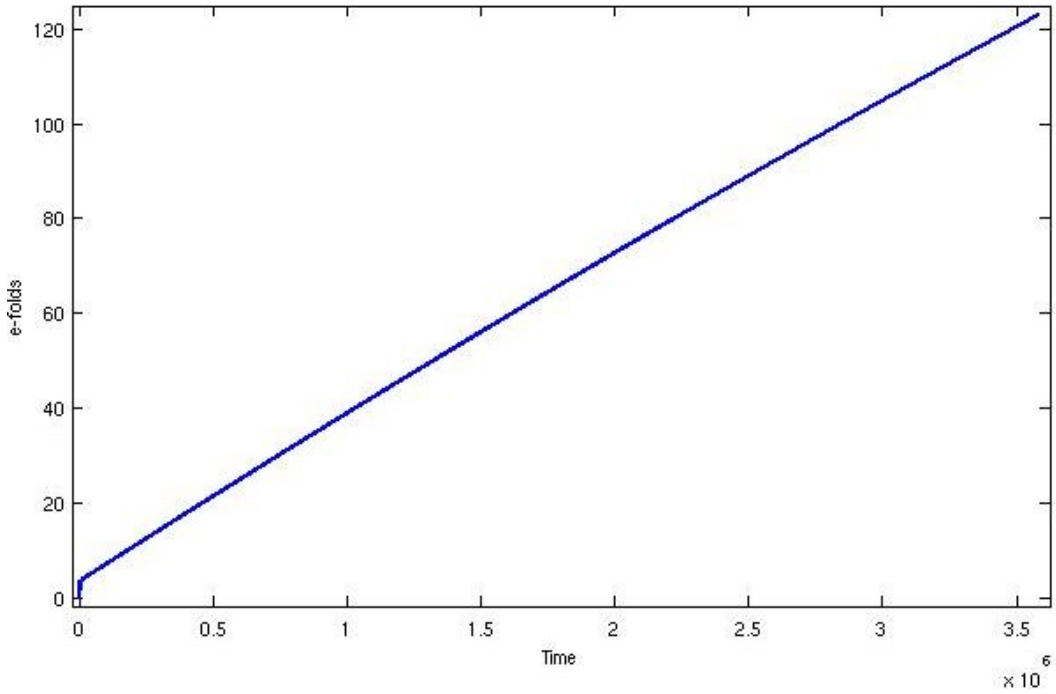

Figure 4.8. efolds against time subject to quartic potential - again we see a long period of slow roll inflation

.

In figure 4.8 we see that we do once again recover a period of slow roll inflation. This simulation began with $\phi_b = 16$ and the evolution of the scalar field can be seen in figure 4.9.

.

Obviously the allowed range of ϕ is restricted by this potential, and from numerical simulations one does indeed recover more than 68 e-folds for $\phi > 10$.

One can further make heuristic arguments about the robustness of our results in the presence of generic potentials. The quadratic and quartic potentials exhibit enough inflation when ϕ_b is relatively close to the minimum of the potential and moving towards the minimum. In these cases the Hubble parameter is zero, therefore we have the least possible friction. In a more general setting we can consider the trajectory of the scalar field subject to a more complicated potential which is approximated by a quadratic or quartic in the vicinity of its minimum. Let us

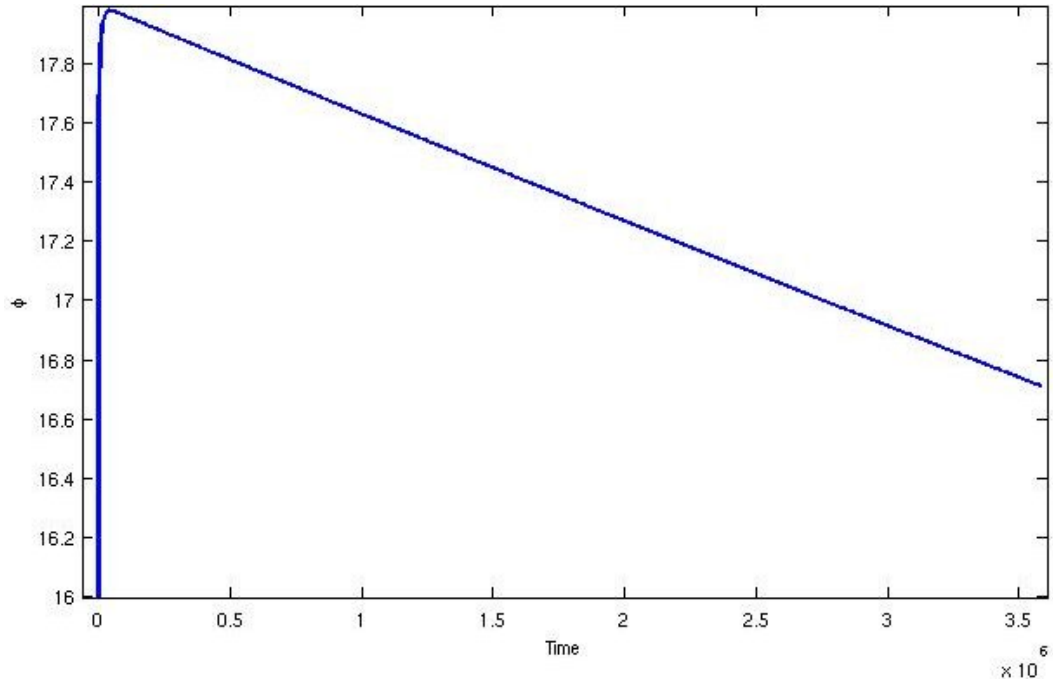

Figure 4.9. Evolution of inflaton subject to quartic potential - despite the new form of potential the slow roll behavior persists.

suppose this approximation holds for, say, $\phi - \phi_o < 10$ where ϕ_o are the locations of the minima of the potential, where we shall take the potential to be zero to exclude the deSitter cases which will obviously lead to enough efolds. Then, any motion of ϕ outside these regions will eventually encounter one of these regions. At such time, the Hubble parameter will be non-zero, and the energy density lower than the bounce density. Therefore in these regions the inflaton will be moving slower than if it had begun its motion in this region, and will encounter (at least initally) more friction, and thus we are likely to see more efolds. Therefore it is likely that the results we have obtained will hold for a general class of potentials, not just the quadratic or quartics considered so far. However it should be stressed that this is a heurestic argument only and further study is required to establish these results in any detail.

4.6 Probability of Inflation

In this section we will define a measure on the space of solutions to our theory. We will then define the *a priori* probability of an event occurring as being the volume of the space of solutions in which the event occurs, where the total volume of the space of solutions has been normalized to unity. This idea arises as Laplace's Principle of Indifference which states that in the absence of further information, if an observation can have N possible outcomes one should assign equal probability $(1/N)$ to each. In the case we consider there is not a discrete set of outcomes but rather a continuum, and hence a measure on this space must be employed to perform such a counting operation.

4.6.1 Defining Probabilities

A natural measure available on phase space is the *Liouville Measure* $d\mu_L$. A volume form is obtained on a D-dimensional phase space by taking the symplectic structure ω and raising it to the power $D/2$ (Note here that D is even by virtue of each configuration variable having a conjugate momentum). Thus we are equipped with a volume form $\Omega = \omega^{D/2}$ on phase space. Since we are interested in *solutions* to our theory we must find a surface S within phase space which every solution crosses exactly once, and define our measure on the space of solutions, Ω_s to be the pull-back of Ω to this surface.

We can therefore define the *a priori* probability of an event X occurring to be:

$$P(X) = \frac{\int_A \Omega_s}{\int_S \Omega_s} \tag{4.22}$$

Where A is the subset of solutions in S for which the event X occurs. Since the Liouville measure is preserved under evolution, it does not matter which surface S we choose so long as each solution crosses it exactly once. At this point, one might be tempted to point out that we have merely a measure on this space, and that by introducing a probability density function f on the surface S one could obtain

$$P'(X) = \frac{\int_A f(u)\Omega_s}{\int_S f(u)\Omega_s} \tag{4.23}$$

where P' is the probability as defined with reference to this density function,

and u some variables on S. To answer this question we must introduce the notion of the *Information* contained in a probability density function.

The information contained in a probability density function $f(u)$ is defined to be

$$I = \int f(u) ln(f(u)) du \tag{4.24}$$

under the constraint that the total probability be normalized to 1 and be positive for all u. The information I is minimized by the uniform distribution, $f(u) = 1$, and hence we are justified in choosing 4.22 to be our definition of *a priori* probability. Furthermore it can be seen that such *a priori* probabilities are of particular interest when they are particularly low. In these cases there is a heavy burden placed upon any theory to provide sufficient information to overcome this bare probability.

4.6.2 Harmonic Oscillator

Once we have a total measure which is finite, we can ask questions about probabilities of our system having certain physical properties, or the moments (expectation values) of our variables. To find the probability that our system has a certain property, X we need to identify the portion of phase space A which corresponds to this property.

In order to better understand what is going on here, let us investigate the canonical physics test problem: The harmonic oscillator. To have the same number of degrees of freedom, let us consider a 2D SHO with a given energy E with unit mass and spring constant. The task will be to investigate the likelihood of the oscillator having certain physical properties without being given any further information about its state. We can proceed using the above method:

The expressed in polar coordinates, our constraint is

$$C = 2E - P_r^2 - \frac{P_\phi^2}{r^2} + r^2 \tag{4.25}$$

With symplectic structure

$$\omega = dP_r \wedge dr + dP_\phi \wedge d\phi \tag{4.26}$$

Here we have options in terms of which slicing we choose in order to count the number of solutions. Note that each solution crossed $P_r = 0$ at least twice on an orbit, at the minimum and maximum values of r. This might indicate that we should use $r = r_{min}$ and P_r to define the surface onto which we pull back the symplectic structure. However, we have far more powerful tools at our disposal in this case: we know that P_ϕ is a constant of motion and that the constraint is independent of ϕ. Therefore a simpler method is to eliminate P_r using our constraint, and pullback onto a $\phi = constant$ surface.

From our constraint

$$P_r = \sqrt{2E - \frac{P_\phi^2}{r^2} - r^2} \tag{4.27}$$

and hence our natural two-form is:

$$\overleftarrow{\omega} = \frac{2P_\phi}{\sqrt{2E - \frac{P_\phi^2}{r^2} - r^2}} dP_\phi \wedge dr \tag{4.28}$$

With the available phase space, $\mathcal{I}$ being

$$P_\phi \in [0, r\sqrt{2E - r^2}], r \in [0, \sqrt{2E}] \tag{4.29}$$

Hence we can integrate our two form over this surface to find the total measure to be $E^2\pi/2$

We can now find expectation values for our physical variables:

$$< P_\phi > = \frac{2}{E^2\pi} \int_{\mathcal{I}} P_\phi \frac{2P_\phi}{\sqrt{2E - \frac{P_\phi^2}{r^2} - r^2}} dP_\phi dr \tag{4.30}$$

$$= \frac{2E}{3} \tag{4.31}$$

And variance

$$< P_\phi >^2 - < P_\phi^2 >= \frac{E^2}{18} \tag{4.32}$$

Likewise we can find the probability that the particle is less than half-way to its maximum radius.

$$P(r < \frac{\sqrt{2E}}{2}) = \frac{2}{E^2\pi}\int_0^{\frac{\sqrt{2E}}{2}} \frac{2P_\phi}{\sqrt{2E - \frac{P_\phi^2}{r^2} - r^2}} dP_\phi dr \tag{4.33}$$

$$= \frac{1}{3} - \frac{\sqrt{3}}{4\pi} \approx 0.2 \tag{4.34}$$

The probability that the particle is within a fraction f of its maximum radius is:

$$P(r < f\sqrt{2E}) = \frac{2}{E^2\pi}\int_0^{f\sqrt{2E}} \frac{2P_\phi}{\sqrt{2E - \frac{P_\phi^2}{r^2} - r^2}} dP_\phi dr \tag{4.35}$$

$$= \frac{2f\sqrt{1-f^2}(2f^2-1) + ArcSin(f)}{\pi} \tag{4.36}$$

From which we find the pleasant result that $P(r < f\sqrt{2E}) = 0.5$ for $f = 2^{-\frac{1}{2}}$.

So, what about a more difficult yet physically relevant quantity? As an example, let us consider the shape of the ellipse described by the particle, in particular let us consider:

$$e = \frac{r_{min}}{r_{max}} \tag{4.37}$$

As written this is not easily found using the methods described. In order to find this quantity let us exploit a further set of tools at our disposal: The equations of motion. Finding the min and max values of r we want to use the condition $\dot{r} = 0$. Using the equations of motion, this tells us that $P_r = 0$. On the surface of solutions to our constraint this then tells us:

$$\frac{P_\phi}{2r^2} + \frac{r^2}{2} = E \tag{4.38}$$

and setting $u = r^2$ and noting that there is only one physical solution to this with r being the positive square root, we then find that these values are solutions

to the equation:

$$u^2 - 2uE + P_\phi^2 = 0 \tag{4.39}$$

We then find the shape parameter to be

$$e = \sqrt{\frac{1 - \sqrt{1 - \frac{P_\phi^2}{E^2}}}{1 + \sqrt{1 - \frac{P_\phi^2}{E^2}}}} \tag{4.40}$$

If we want to find out if our orbits are almost circular we can then integrate our measure from $e = e_0$ to $e = 1$. We set $v = \sqrt{1 - \frac{P_\phi^2}{E^2}}$. Then for small v we find: $e \approx 1 - v$, and hence we integrate our measure from $P_\phi = E\sqrt{2e_0 - e_0^2}$ to $P_\phi = E$ and over the region $r_{min} < r < r_{max}$.

By numerical methods we find that the probability of being in an orbit with shape parameter $e > 0.5$ to be around 0.2 and hence would conclude that orbits which appear circular are very unlikely.

4.6.3 Application to Inflation

Let us now apply this procedure to the system in question. We form the Liouville measure $\Omega = dP_\phi \wedge d\phi \wedge db \wedge d\nu$. Recall that we have a single Hamiltonian constraint to satisfy and from our equations of motion b is monotonic decreasing on any open interval in time with no fixed points on the interval $(0, \pi/\lambda)$ and hence for any b_0 in this interval every solution crosses $b = b_0$ exactly once. In particular, since we are interested in knowing probabilities for numbers of efolds *after* the bounce, we can pick the bounce point, $b = \pi/2\lambda$ to define our surface.

$$S = \{H = 0\} \cap \{b = \frac{\pi}{2\lambda}\} \tag{4.41}$$

Note that this choice for b is made purely for ease of calculation. The results obtained are independent of this choice due to the invariance of the Liouville measure. We further solve the Hamiltonian constraint to eliminate P_ϕ leaving the measure on this surface:

$$\Omega_s = \sqrt{\frac{3\pi}{\lambda^2} - 8\pi^2\gamma^2 V(\phi)}d\nu \wedge d\phi \tag{4.42}$$

In the above expression the square root is necessarily real on the set of solutions to the Hamiltonian constraint, since the potential cannot exceed the critical density. We are now in a position to calculate the total measure

$$N = \int_S \Omega_s \tag{4.43}$$

Here we notice that the surface S is non-compact and therefore the total measure is in fact infinite. The problem arises because we are considering the space of all possible volumes, ν at the bounce point. However, as has been previously mentioned, there is no *physical* meaning to this quantity in the $k = 0$ case, as choice of volume at a given point can be considered gauge. Therefore, since our task is to count the number of *physically distinct* solutions, we should take the further step of eliminating this choice. This can be done in a number of ways; One can perform a group-averaging procedure under the action of rescaling the volume, place a cut-off on any integral over volume and take the limit as we relax this cut-off, or declare the fiducial cell used to be that which gives the volume at the bounce to be a fixed value, say $\nu_b = 1$. Performing any one of these leaves the same result in terms of a priori probability of physical events, since we have fixed this gauge degree of freedom leaving us with a system entirely determined by the value of the inflaton at the bounce point, ϕ_b. Thus we derive the probability that the value of the scalar field lies in a set A at the bounce point to be

$$P(\phi_b \in A) = \frac{1}{N}\int_{\phi\in A} \sqrt{\frac{3\pi}{\lambda^2} - 8\pi^2\gamma^2 V(\phi)}d\phi \tag{4.44}$$

wherein N is the total measure on this space:

$$N = \int_S \sqrt{\frac{3\pi}{\lambda^2} - 8\pi^2\gamma^2 V(\phi)}d\phi \tag{4.45}$$

and S the region $V(\phi) < \rho_c$ (in which the square root takes real values). The total measure is finite if we enforce weak restrictions on $V(\phi)$: that it be bounded

below and the region $V(\phi) < \rho_{\text{crit}}$ is compact[3] we have a finite total measure, and well defined notion of probability.

4.6.4 The Quadratic Potential

Let us now focus our attention on the quadratic potential $V(\phi) = m^2\phi^2/2$. This potential satisfies all the requirements outlined above, namely it is bounded below and the region in which the energy density is less than the critical density is compact. In particular the value of the inflaton at the bounce must be in the region $S = [-\sqrt{2}\rho_{\text{crit}}/m, \sqrt{2}\rho_{\text{crit}}/m]$.

The procedures outlined above now yield a finite total measure N given by

$$N = \int_S \sqrt{\frac{3\pi}{\lambda^2} - 4\pi^2\gamma^2 m^2\phi^2} d\phi = \frac{3\pi}{4\gamma\lambda^2 m} \tag{4.46}$$

We are now in a position to calculate the a priori probability of the inflaton being in a certain region at the bounce point, whose relationship to the number of efolds a solution will undergo has been previously established.

We can state the cumulative distribution function, $P(\phi_b) \in [0, f\phi_{max}]$, where ϕ_{max} is the value of ϕ such that $V(\phi) = \rho_{\text{crit}}$, as

$$\frac{2}{\pi}(f\sqrt{1-f^2} + sin^{-1}(f)) \tag{4.47}$$

From the details of 4.4 we see that the only cases in which we do *not* see 68 efolds of inflation is that of strong kinetic domination with f in the range $[-3.5*10^{-7}, 6.6*10^{-7}]$. From our cumulative distribution function we find that the probability that we are indeed on one of these trajectories is $6.4 * 10^{-6}$. Therefore the *a priori* probability that we see 68 efolds of inflation in LQC coupled to a massive scalar field is very high meaning that in this system it would take a great deal of fine tuning to *avoid* inflation.

This result holds under an increase of the inflaton mass by up to two orders of magnitude (ie $m < 6 * 10^{-5} m_{pl}$). At this value, the range of f which leads to less than 68 efolds is $[-3.1 * 10^{-4}, 1.1 * 10^{-4}$ and hence the *a priori* probability that we find the inflaton in this range at the bounce is $2.7 * 10^{-4}]$, again giving us a greater

[3]This condition is non-restrictive in the sense that all polynomials with even leading powers will satisfy it

than 99.9% chance of seeing 68 efolds. Under a decrease in the inflaton mass, the probability of 68 efolds increases until the inflaton mass becomes zero.

4.6.5 The Quartic Potential

As discussed above 4.5 a more generic potential for the inflaton can be considered. In the case examined here, we see that from numerical simulations we recover 68 efolds when $|\phi_b| > 10$. Hence we can repeat the process above and calculate the probability of being in this region. There is also a region around $\phi = 0$ which is an unstable equilibrium point on our potential, and will contribute to the set that leads to at least 68 e-folds. However, we can gain a crude lower bound by ignoring this region.

To simplify the calculation, we will consider only the pure quartic contribution. This will actually reduce our allowed range of ϕ contributing to our crude lower bound. In doing this we find the probability of ϕ_b being less than some fraction f' of its maximum to be

$$P[\phi_b < f'\phi_{max}] = \frac{5p * \Gamma(7/4)_2F_1[-1/2, 1/4, 5/4, p^4]}{2\sqrt{\pi}\Gamma(9/4)} \tag{4.48}$$

and we once again recover a greater than 99.9% probability of seeing 68 efolds.

4.6.6 Alternate Start Point

One can take the viewpoint that instead of beginning our count of the number of efolds at the bounce point, one should rather begin at some point at which GR is valid. In LQC this can be taken to correspond to the density being around 1% of the critical density. Here for simplicity we will consider only the quadratic potential case, with analogous arguments holding for quartic potentials. Then, following the above prescriptions, one can calculate the fraction of solutions which undergo 68 efolds from this point forwards. There are two fundamental differences between this formulation and that considered at the bounce point: The first is that there will be no superinflation in this counting. Since the density is well below the critical density the Hubble parameter H is monotonic non-increasing from this point forward, which is a consequence of being in good agreement with

the dynamics of GR. The second is that the allowed region on phase space is smaller - we consider S' to be the region in which $V(\phi) < 0.01\rho_{\rm crit}$. This in turn reduces ϕ_{max} by a factor of 10. In doing so, we recover exactly the same probability distribution in terms of $f = \phi/\phi_{max}$ as before, however the region which leads to more than 68 efolds has changed.

From numerical simulations we find that the region in which we do not see 68 efolds of inflation is $\phi_{\rho=0.01\rho_{\rm crit}} \in [-5, 3]$. This again corresponds to a greater than 99.9% chance of seeing at least 68 efolds of inflation forwards of this time, although it is indeed lower than the estimate beginning at the bounce. Since the Liouville measure is preserved under evolution, if we counted again the number of solutions in which we see 68 efolds from the bounce point, we would indeed recover the same result. The difference here is precisely the portion of trajectories in which we see less than 68 efolds after reaching 1% of the critical density yet more than 68 from the bounce point.

4.7 Discussion

Although highly successful as an explanation for physical phenomena, the inflationary scenario in GR encounters a number of conceptual difficulties. Questions about whether inflation is a generic phenomenon arise, and the framework is not equipped with the tools to answer these questions. Similarly the total number of efolds is an ill-defined quantity, as an expanding cosmological solution begins with a big bang in which the Hubble parameter and matter density are infinite, and volume zero. These importance of these issues is amplified by the success of inflation.

In this chapter we examined the effects of the LQC corrections to GR. Expanding cosmology now begins at a bounce point, with zero Hubble parameter, fixed finite density and a non-zero volume. We have seen that LQC yields a paradigm in which questions of inflation can be made precise: The bounce gives a clear 'start point' from which to count efolds, and we can form a natural measure on phase space which shows that in a somewhat general inflationary scenario, the *a priori* probability of the universe undergoing enough efolds to solve physical problems is very high. This in turn indicates that the inflationary scenario in LQC does not

require 'fine tuning', but rather that the *generic* predictions of the model are in good agreement with the observed data.

This is not to say that all the problems of inflation are addressed in LQC. LQC has so far put forward no candidate field to play the role of the inflaton, the scalar field used here was added by hand for the purpose. One possible candidate under consideration is the taking the Barbero-Immirzi parameter γ to be a field [64]. However, in this case the dynamics of the associated quantum cosmology have yet to be defined and would likely be different from those described here, not least because the critical density depends directly upon this parameter. It is also assumed that the inflaton somehow decays into other matter fields which go on to become the constituents of our observed universe. Again there is no detailed model for this decay, only the idea that around the minimum of the potential this is expected to occur. The scalar field can be thought of as merely a model for the inflaton, whose dynamics are in reality described by a more complicated system. As was noted above, the scalar field changes equation of state across all non-phantom matter and so is a good toy model for more complicated dynamics, especially once more complicated potentials are considered.

A second question which arises is that of the 'trans-planckian' nature of a cosmology which undergoes a large degree of inflation. If, as is highly likely according to our measure, the universe underwent a large number of efolds (say > 150) then at the bounce point the entire currently observable universe would have had a radius less than the planck length. Therefore one could argue that quantum fluctuations of the fields involved, which could be large at the bounce, should still be present and so the universe would not appear classical. This argument is somewhat vague, as in all singular cosmologies there is point beyond which the entire observable universe would be less than a plank length in radius. Inflation does highlight this problem as rapid expansion would cause this region to expand more quickly, but this question appears one that should be addressed by cosmology as a whole, not simply inflationary models.

Inflation, as was shown in chapter 3 is a generic feature of LQC. The particular model of inflation due to a scalar field being subject to a potential has a high probability of producing a universe which agrees with cosmological observations. Therefore we find the opposite result to that of Gibbons and Turok - it would

require fine tuning to have an inflationary universe which did *not* produce enough inflation.

Appendix A

Numerical Details of BKL Simulations

A.1 One point evolutions

Simulations of the BKL system for a single set of initial data described by 2.59 and 2.58 were performed in MATLAB using a Runge-Kutta (4,5) algorithm (ODE45) [65] to numerically solve the differential equations. Both relative and absolute tolerances were set at 10^{-14} and on every solution preservation of the Hamiltonian constraint 2.57 to this order was verified. Calculations of the u-map and Hamiltonian were performed on the raw output data. In both the simulations done on the BKL conjecture and the inflationary trajectories in LQC, we are evolving a Hamiltonian system. Numerical error in the system is not directly coupled to any of the dynamical variables, and therefore will play the role of a cosmological constant (which is pseudo-random in time). In requiring that the absolute tolerance levels of our system are small in comparison to the timescales involved, we ensure that the integrated effect over time of this error is small - the effective cosmological constant created by this error plays little role in long term evolution. In also requiring that the relative tolerance for error is low we ensure that there is little effect played by the change of this parameter, hence our solutions do in fact well approximate the physical systems after which they are modeled.

A.1.1 The u-map

Through numerical simulation we are able to verify the behavior of the u-map as state in 2.80 - we do see the signature stepping down by 1 of the u parameter and its inversion below 2 in systems which have settled into a Bianchi I/Bianchi II transition regime. However, at early times this behavior is not necessarily present - it is a phenomenon which can appear in our simulations at late times, as we see in figures A.1 and A.2

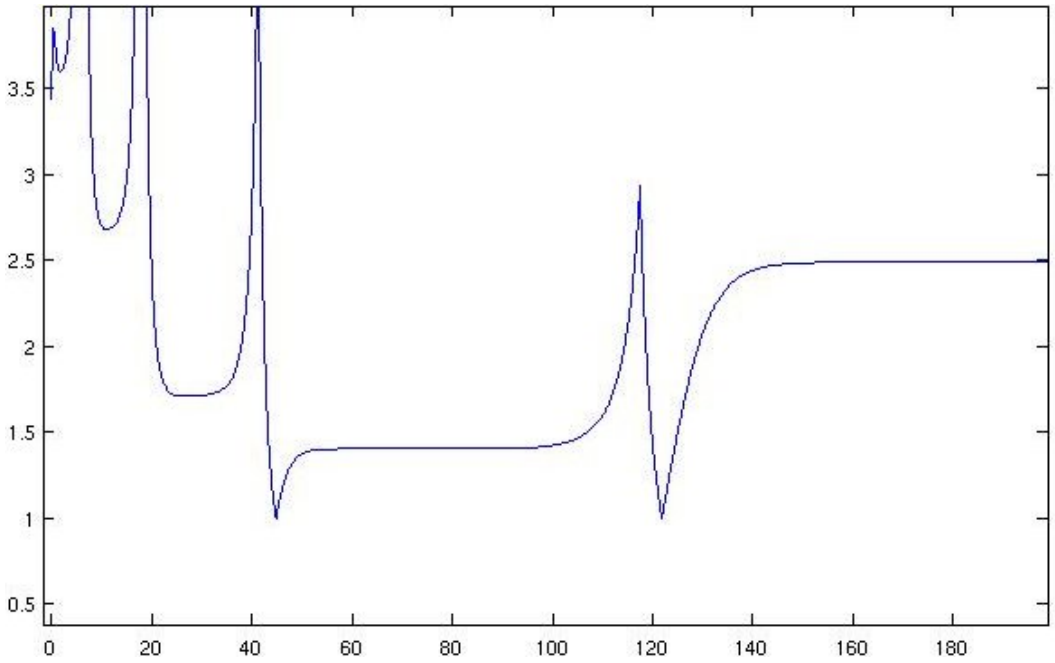

Figure A.1. The system can quickly settle into u-map behavior when starting from an almost Kasner state

Adding a scalar field to the system stops this behavior - the u-map appears to be no longer valid when there is matter present. This is clearly to be expected as the presence of a strong enough scalar field, as discussed in chapter 2, causes the Taub transitions to cease. An example of this is shown in figure A.3.

A.1.2 Function fitting

The approximation of our solutions by a sum of *sech* functions was also performed numerically. For each Taub transition, the fitting was asigned two parameters

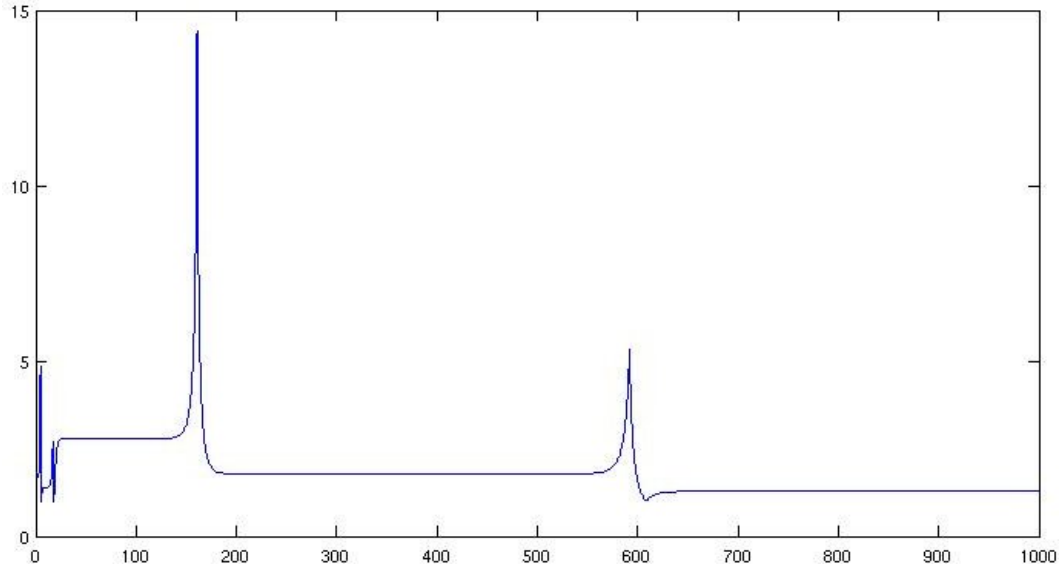

Figure A.2. A system initially far from a Kasner state can require some initial 'settling' before the u-map behavior emerges

corresponding to the amplitude and time of the *sech* function used in the approximation. The initial positions for the search on the space of functions were the peak points of the transitions. These were then fit to the data using an multivariate linear fitting program (nlinfit).

In this simulation we observe that even when the number of transitions is far higher than the number of degrees of freedom in the system we still can recover a close approximation to the dynamics. Here there are several transitions in the highest eigenvalue of C which appear to be perturbations around the one more long term transition which is well fit by the associated *sech* function.

A.2 Solutions with varying initial data

In order to investigate the presence of spikes in our system it was necessary to perform simulations in which the initial data varied over space such that a spike would form during a Taub transition. These simulations were run on hand written differential equation solving code using an iterative Picard method to solve the equations. Despite the calculational inefficiency of using superlinear methods over increasing data points, memory limitations of the systems involved caused

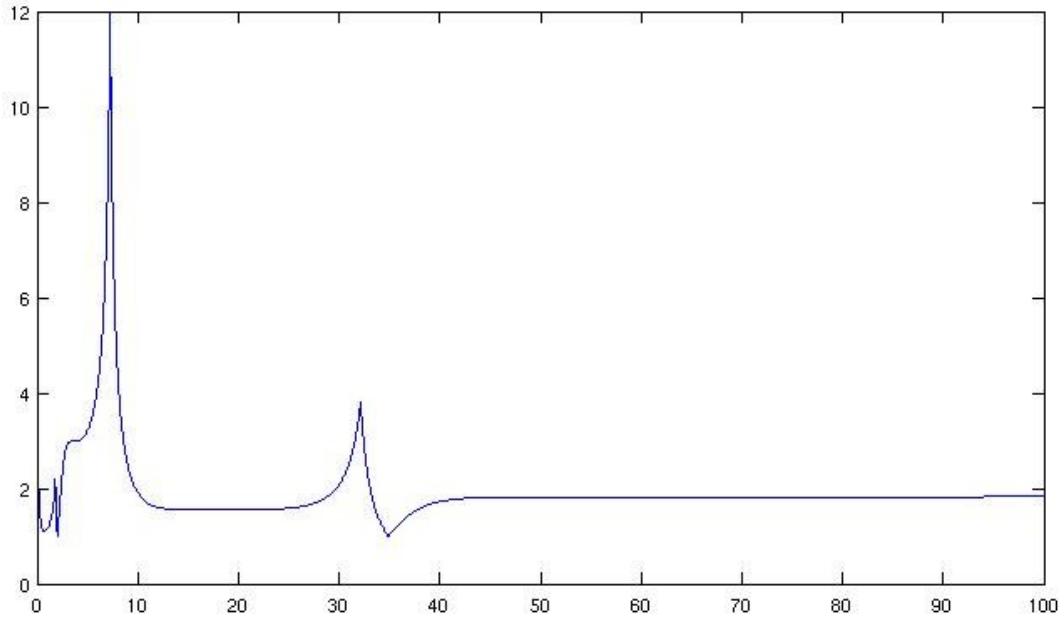

Figure A.3. The non u-map behavior in the presence of a scalar field. Here the scalar field is not strong enough to stop transitions but does break the u-map

optimization of the grid beyond a certain point (around 10^6 grid points) to be impossible. Therefore once an optimal grid was achieved the number of iterations of the Picard algorithm was increased.

Initial data was picked by choosing the all three eigenvalues of P and one of C. The second eigenvalue of C was varied across the allowed parameter space and the Hamiltonian constraint applied to solve for the remaining eigenvalue. In doing so we ensured that all our initial data satisfied the boundary conditions imposed and that we were indeed evolving physical solutions to our theory.

In figure A.5 we see an example of the behavior of a spike in the eigenvalue of C. Here we see that on either side of the 'spike point' transitions occur, one with positive C the other negative. The spike point itself is actually stationary as no transition occurs at this point. It is rather the nearby transitions that pick out this point, as the nearby eigenvalues diverge.

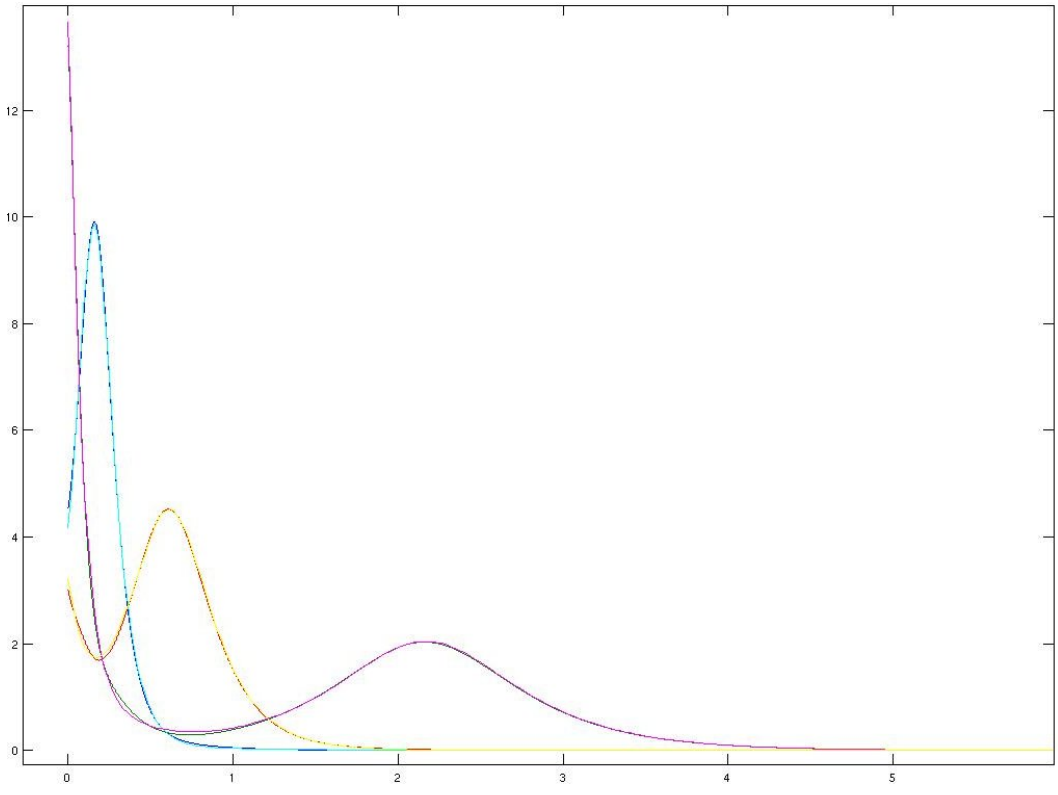

Figure A.4. Fit of varied C evolution by sum of sech functions

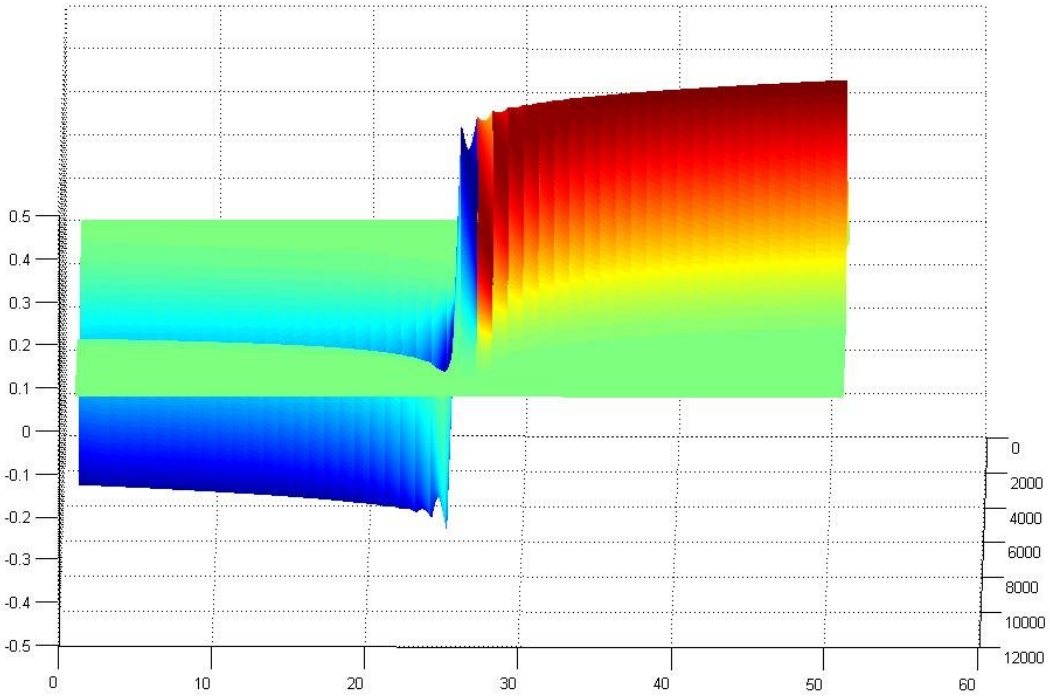

Figure A.5. Profile view of spike in C

Appendix B

Numerical Details of LQC Simulations

Simulations of the LQC inflationary system for a single set of initial data described by 4.3-4.6 were performed in MATLAB using a variable order Adams-Bashforth-Moulton PECE solver (ODE113)[66] to numerically solve the differential equations. In the simulations for precision the natural logarithm of the volume was taken as a fundamental variable instead of the volume itself. Both relative and absolute tolerances were set at 10^{-14} and on every solution preservation of the Hamiltonian constraint 4.1 to this order was verified. Simulations all used the choice that the volume at the bounce point, ν_b was fixed to unity, and initial conditions were fixed by choice of the value of the scalar field ϕ, with the Hamiltonian 4.1 being used to calculate p_ϕ. Since our system is symmetric under $\phi, p_\phi \to -\phi, -p_\phi$ we could, without loss of generality, take the positive square root that arose from solving the constraint.

Upon completion of a simulation the various physical quantities of interest (in particular the number of efolds) were calculated. This was done numerically, performing a binary search for the maxima of ϕ to establish turning points, and for $\ddot{\phi}$ for the onset of slow-roll inflation. Similarly a search of where ϕ exited slow-roll was calculated numerically, with the exit point being the point where the slow roll conditions were violated. A spot check of these results was performed by hand for generic statements, and any individual results required were verified directly.

As a test case for every simulation, both the massless scalar field and fixed

potential (effective cosmological constant) solutions were calculated and compared to their known analytic solutions. In each case agreement up to one part in a million were observed in the evolutions of the fundamental variables. Similarly simulations in which the initial volume was varied by orders of magnitude in each direction were performed, producing identical results to the case in which the volume was fixed. Likewise the negative p_ϕ solution to the Hamiltonian constraint was checked to yield identical physical results to the positive choice. This is obvious from a physical perspective, however from the point of view of simulations it was necessary to establish that no artifacts of our choices of gauge were present in the simulations themselves.

In order to establish the data for 4.1 a preliminary search on the initial parameter space of ϕ was performed with a uniform linear spacing between data points. Once this revealed the approximate location of the minimum, a binary search on this space was performed until the minimum of the number of efolds as a function of initial parameter was found and verified to 3 significant figures.

Numerical simulations were used to find the number of efolds directly only in the kinetic dominated case. Once the number of efolds grew beyond 100 the numerical stability of the equations would break. Fortunately, at this point we were beyond the point of interest in our paradigm, since we are interested in initial conditions which yield less than 68 efolds. In both the intermediate and potential dominated regimes, the numerical solutions were used to verify that this bound was exceeded.

Bibliography

[1] S. Hawking and G. Ellis The Large Scale Structure of Space-Time Cambridge University Press 1973

[2] T. Sotiriou and V. Faraoni $f(R)$ Theories of Gravity Rev. Mod. Phys. **82** 451 2010

[3] A. Friedmann ber die Mglichkeit Einer Welt mit Konstanter Negativer Krmmung des Raumes Zeitschrift fr Physik **21** 326 1924.

[4] G. Lemaitre Un Univers Homogne de Masse Constante et de Rayon Croissant Rendant Compte de la Vitesse Radiale des Nbuleuses Extragalactiques Annales de la Socit Scientifique de Bruxelles 1927

[5] H. Robertson Kinematics and World Structure Astrophys. J. **82** 248 1935

[6] A. Walker On Milnes Theory of World-Structure Proc. Lon. Math. Soc. 2 **42** 90 1937

[7] J. Allday Quarks, Leptons and the Big Bang Insitute of Physics Press 2002

[8] A. Sakharov Violation of CP Invariance, C Asymmetry, and Baryon Asymmetry of the Universe. J. Exp. and Theor. Phys. **5** 24 1967

[9] G. Steigman Primordial Nucleosynthesis in the Precision Cosmology Era. Ann. Rev. Nuc. Part. Sci. **57** 463

[10] C. Rolfs and W. Rodney Cauldrons in the Cosmos Univ. of Chicago Press 1988

[11] A. Ashtekar, A. Henderson and D. Sloan Hamiltonian General Relativity and the Belinskii, Khalatnikov, Lifshitz Conjecture Class. Quant. Grav. **26** 052001 2009

[12] I. Khalatnikov and E. Lifshitz General Cosmological Solution of the Gravitational Equations with a Singularity in Time, Phys. Rev. Lett. **24** 1970

[13] L. Bianchi, Sugli spazii a tre dimensioni che ammettono un gruppo continuo di movimenti. Soc. Ital. Sci. Mem. di Mat. **11** 267 1898

[14] B. Berger Living Reviews in Relativity **1** 2002

[15] D. Garfinkle Numerical Simulations of Generic Singuarities Phys.Rev.Lett. **93** 161101 2004

[16] B. Berger and V. Moncrief Numerical Investigation of Cosmological Singularities Phys.Rev. D**48** 4676 1993

[17] B. Berger, D. Garfinkle, J. Isenberg, V. Moncrief and M. Weaver The Singularity in Generic Gravitational Collapse Is Spacelike, Local, and Oscillatory Mod. Phys. Lett. A**13** 1565 (1998)

[18] M. Weaver, J. Isenberg and B. Berger Mixmaster Behavior in Inhomogeneous Cosmological Spacetimes Phys.Rev.Lett. **80** 2984 1998

[19] L. Anderson and A. Rendall Quiescent cosmological singularities Commun. Math. Phys **218** 479 2001

[20] B. Berger and V. Moncrief Numerical Evidence that the Singularity in Polarized U(1) Symmetric Cosmologies on $T^3 \times R$ is Velocity Dominated Phys.Rev. D **57** 7235 1998

[21] B. Berger and V. Moncrief Exact U(1) symmetric cosmologies with local Mixmaster dynamics Phys.Rev. D**62** 023509 2000

[22] J.M. Heinzle, C. Uggla, and N. Rohr The Cosmological Billiard Attractor, Adv.Theor.Math.Phys.13 293 2009

[23] J.D Romano Geometrodynamics Vs. Connection Dynamics Gen.Rel.Grav. **25** 759 1993

[24] C. Uggla H. van Elst, J. Wainwrightand G. Ellis The Past Attractor in Inhomogeneous Cosmology Phys. Rev. **D** 68 103502 2003

[25] C. Uggla The Nature of Generic Cosmological Singularity arXiv:0706.0463

[26] M. Heinzle and C. Uggle Mixmaster: Fact and Belief Class. Quant. Grav. **26** 075016 2009

[27] A. Rendall Global Dynamics of the Mixmaster Model Class. Quantum Grav., 14, 2341-2356, (1997)

[28] W. Lim New Explicit Spike Solution – Non-local Component of the Generalized Mixmaster Attractor Class.Quant.Grav.25 045014 2008

[29] R. Wald General Relativity Univ. of Chicago Press 1984

[30] M. Bojowald Loop Quantum Cosmology I:Kinematics Class. Quant. Grav. **17** 1489 2000

[31] M. Bojowald Loop Quantum Cosmology II: Volume Operators Class. Quant. Grav. **17** 1509 2000

[32] M. Bojowald Loop Quantum Cosmology III: Wheeler-DeWitt Operators Class. Quant. Grav. **18** 1055 2001

[33] M. Bojowald Loop Quantum Cosmology IV: Discrete Time Evolution Class. Quant. Grav. **18** 1071 2001

[34] A. Ashtekar and J. Lewandowski Background Independent Quantum Gravity: A Status Report Class. Quant. Grav. **21** R53 2004

[35] M. Bojowald Absence of Singularity in Loop Quantum Cosmology Phys. Rev. Lett. **86** 5227 2001

[36] A. Ashtekar, T. Pawlowski and P. Singh Quantum Nature of the Big Bang Phys. Rev. Lett. **96** 141301 2006

[37] A. Ashtekar, T. Pawlowski, P. Singh and K. Vandersloot Loop Quantum Cosmology of k=1 FRW models Phys. Rev. D**75** 024035 2007

[38] K. Vandersloot Loop Quantum Cosmology and the k = - 1 RW Model Phys. Rev. D**75** 023523 2007

[39] A. Ashtekar and E. Wilson-Ewing Loop Quantum Cosmology of Bianchi I Models Phys. Rev. D**79** 083535 2009

[40] A. Ashtekar and E. Wilson-Ewing Loop Quantum Cosmology of Bianchi Type II Models Phys. Rev. D**80** 123532 2009

[41] G. Mena Marugan and M. Martin-Benito Hybrid Quantum Cosmology: Combining Loop and Fock Quantizations Int. J. Mod. Phys. A**24** 2820 2009

[42] P. Singh Are Loop Quantum Cosmos Never Singular? Class. Quant. Grav. 26 125005 2009

[43] A. Ashtekar, J. Baez, A. Corichi and K. Krasnov Quantum Geometry and Black Hole Entropy Phys. Rev. Lett. **80** 904 1998

[44] I. Agullo, J. Diaz-Polo and E. Frenandez-Borja Black Hole State Degeneracy in Loop Quantum Gravity Phys. Rev. D**77** 104024 2008

[45] V. Taveras Corrections to the Friedmann Equations from LQG for a Universe with a Free Scalar Field Phys. Rev. D**78** 064072 2008

[46] M. Bojowald, D. Mulryne, W. Nelson and R. Tavakol The high-density regime of kinetic-dominated loop quantum cosmology arXiv:1004.3979 2010

[47] A. Ashtekar and T. Schilling Geometrical Formulation of Quantum Mechanics arXiv:gr-qc/9706069 1997

[48] A. Ashtekar, A. Corichi and P. Singh Robustness of Key Features of Loop Quantum Cosmology Phys. Rev. D**77** 024046 2008

[49] M. Bojowald Inflation from Quantum Geometry Phys. Rev. Lett. **89** 261301 2002

[50] E. Copeland, D. Mulryne, N. Nunes and M. Shaeri Super-inflation in Loop Quantum Cosmology Phys. Rev. **D** 77 023510 2008

[51] A. Ashtekar and E. Wilson-Ewing The Covariant Entropy Bound and Loop Quantum Cosmology Phys. Rev. **D** 78 064047 2008

[52] G. Gibbons and N. Turok The Measure Problem in Cosmology Phys. Rev. D**77** 063516 2008

[53] A. Ashtekar and D. Sloan Loop Quantum Cosmology and Slow Roll Inflation arXiv:0912.4093 2009

[54] A. Linde Is the Cosmological Constant Really a Constant JETF Lett. **19** 183 1974

[55] A. Linde Phase Transition in Gauge Theories and Cosmology Rept. Prog. Phys. **42** 389 1997

[56] A. Starobinsky Spectrum of Relict Gravitational Radiation and the Early Stage of the Universe JETP Lett. **30** 719 1979

[57] A. Albrecht and P. Steinhardt Cosmology for Grand Unified Theories with Radiatively Induced Symmetry Breaking Phys. Rev. Lett. **48** 1220 1982

[58] V. Mukhanov CMB-slow, or How to Estimate Cosmological Parameters by Hand Int. J. Theor. Phys. **43** 623 2004

[59] A. Linde A New Inflationary Universe Scenario: A Possible Solution of the Horizon, Flatness, Homogeneity, Isotropy and Primordial Monopole Problems Phys. Lett. B **114** 431 1982

[60] A. Linde Particle Physics and Inflationary Cosmology Contemp. Concepts Phys. **5** 1 2005

[61] S. Hawking The Development of Irregularities in a Single Bubble Inflationary Universe Phys. Lett B **117** 295 1982

[62] A. Guth and S. Pi Phys. Rev. Lett. Fluctuations in the New Inflationary Universe **49** 1110 1982

[63] J. Preskill, Cosmological Production of Superheavy Magnetic Monopoles Phys. Rev. Lett **43** 1365 1979

[64] V. Taveras and N. Yunes The Barbero-Immirzi Parameter as a Scalar Field: K-Inflation from Loop Quantum Gravity? Phys. Rev. D **78** 064070 2008

[65] J Dormand and P. Prince A family of Embedded Runge-Kutta Formulae J. Comp. Appl. Math. **6** 19 1980

[66] L. Shampine. and M. Gordon Computer Solution of Ordinary Differential Equations: The Initial Value Problem W. H. Freeman San Francisco 1975.

Vita

David Sloan

David Sloan was born in Preston, UK on January 26, 1982. He attended St. Peter's College of Oxford University from 2000-2004, graduating with a Master of Mathematics degree (1^{st} class honours). In 2004 he moved to the Pennsylvania State University working in the research group of professor Abhay Ashtekar. Amongst his honors are a Domus Scholarship in Mathematics and the Charles C Caine prize for Mathematics, gained at Oxford, and a gravitational physics fellowship, three Duncan fellowships and two Frymoyer fellowships gained at Penn State. His publications include:

- A. Ashtekar, J. Engle and D. Sloan Asymptotics and Hamiltonians in a First Order Formalism Class. Quant. Grav. **26** 095020 2008
- A. Ashtekar and D. Sloan Action and Hamiltonians in Higher Dimensional General Relativity: First Order Framework Class. Quant. Grav. **25** 225025 2008
- T. Liko and D. Sloan First-order Action and Euclidean Quantum Gravity Class. Quant. Grav. **26** 145004 2009
- A. Ashtekar, A. Henderson and D. Sloan A Hamiltonian Formulation of the BKL Conjecture Class. Quant. Grav. **26** 052001 2009
- A. Randono and D. Sloan The Internal Spin Angular Momentum of an Asymptotically Flat Spacetime Phys. Rev. D **80** 2009
- A. Ashtekar and D. Sloan Loop quantum cosmology and slow roll inflation arXiv:0912.4094 2009